Article (refereed) - postprint

Holmberg, Maria; Aherne, Julian; Austnes, Kari; Beloica, Jelena; De Marco, Alessandra; Dirnböck, Thomas; Fornasier, Maria Francesca; Goergen, Klaus; Futter, Martyn; Lindroos, Antti-Jussi; Krám, Pavel; Neirynck, Johan; Nieminen, Tiina Maileena; Pecka, Tomasz; Posch, Maximilian; Pröll, Gisela; Rowe, Ed C.; Scheuschner, Thomas; Schlutow, Angela; Valinia, Salar; Forsius, Martin. 2018.
Modelling study of soil C, N and pH response to air pollution and climate change using European LTER site observations. *Science of the Total Environment*, 640-641. 387-399. https://doi.org/10.1016/j.scitotenv.2018.05.299

1

Modelling study of soil C, N and pH response to air pollution and climate change using European LTER site observations

Maria Holmberg[1*], Julian Aherne[2], Kari Austnes[3], Jelena Beloica[4], Alessandra De Marco[5], Thomas Dirnböck[6], Maria Francesca Fornasier[7], Klaus Goergen[8,9], Martyn Futter[10], Antti-Jussi Lindroos[11], Pavel Krám[12], Johan Neirynck[13], Tiina Maileena Nieminen[11], Tomasz Pecka[14], Maximilian Posch[15], Gisela Pröll[6], Ed C. Rowe[16], Thomas Scheuschner[17], Angela Schlutow[18], Salar Valinia[3,19], Martin Forsius[1]

[1] Finnish Environment Institute (SYKE), Mechelininkatu 34a, FI-00251 Helsinki, Finland

[2] Environmental and Resource Studies, Trent University, Peterborough, Ontario K9J 7B8, Canada

[3] Norwegian Institute for Water Research NIVA, Gaustadalléen 21, NO-0349 Oslo, Norway

[4] Faculty of Forestry, University of Belgrade, Kneza Viseslava 1, RS-11000 Belgrade, Serbia

[5] ENEA – Casaccia Research Centre, Via Anguillarese 301, IT-00123 Santa Maria di Galeria, Rome, Italy

[6] Environment Agency Austria, Spittelauer Lände 5, A-1090 Vienna, Austria

[7] Institute for Env. Protection and Research (ISPRA), Via Vitaliano Brancati 48, IT-00144 Rome, Italy

[8] Institute of Bio- and Geosciences, Agrosphere (IBG-3), Research Centre Jülich, Jülich, Germany

[9] Centre for High-Performance Scientific Computing in Terrestrial Systems, Geoverbund ABC/J, Jülich, Germany

[10] Swedish University of Agricultural Sciences SLU, P.O. Box 7050, SE-75007 Uppsala, Sweden

[11] Natural Resources Institute Finland LUKE, Latokartanonkaari 9, FI-00790 Helsinki, Finland

[12] Czech Geological Survey, Klárov 3, CZ 11821 Prague, Czech Republic

[13] Research Institute for Nature and Forest (INBO), Gaverstraat 35, BE-9500 Geraardsbergen, Belgium

[14] Institute of Env. Protection – National Research Institute (IOS-PIB) ul. Kolektorska 4, PL-01692 Warsaw, Poland

[15] International Institute for Applied Systems Analysis (IIASA), Schlossplatz 1, A-2361 Laxenburg, Austria

[16] Centre for Ecology and Hydrology (CEH), ECW, Bangor, LL57 3EU, UK

[17] Umweltbundesamt UBA, Wörlitzer Platz 1, DE-06844 Dessau-Roßlau, Germany

[18] ÖKO-DATA Hegermühlenstraße 58, D-15344 Strausberg, Germany

[19] Swedish Environmental Protection Agency, SE-10648 Stockholm, Sweden

[*] email address of corresponding author: maria.holmberg@ymparisto.fi

Abstract

Current climate warming is expected to continue in coming decades, whereas high N deposition may stabilize, in contrast to the clear decrease in S deposition. These pressures have distinctive regional patterns and their resulting impact on soil conditions is modified by local site characteristics. We have applied the VSD+ soil dynamic model to study impacts of deposition and climate change on soil properties, using MetHyd and GrowUp as pre-processors to provide input to VSD+. The single-layer soil model VSD+ accounts for processes of organic C and N turnover, as well as charge and mass balances of elements, cation exchange and base cation weathering. We calibrated VSD+ at 26 ecosystem study sites throughout Europe using observed conditions, and simulated key soil properties: soil solution pH (pH), soil base saturation (BS) and soil organic carbon and nitrogen ratio (C:N) under projected deposition of N and S, and climate warming until 2100. The sites are forested, located in the Mediterranean, forested alpine, Atlantic, continental and boreal regions. They represent the long-term ecological research (LTER) Europe network, including sites of the ICP Forests and ICP Integrated Monitoring (IM) programmes under the UNECE Convention on Long-range Transboundary Air Pollution (LRTAP), providing high quality long-term data on ecosystem response. Simulated future soil conditions improved under projected

decrease in deposition and current climate conditions: higher pH, BS and C:N at 21, 16 and 12 of the sites, respectively. When climate change was included in the scenario analysis, the variability of the results increased. Climate warming resulted in higher simulated pH in most cases, and higher BS and C:N in roughly half of the cases. Especially the increase in C:N was more marked with climate warming. The study illustrates the value of LTER sites for applying models to predict soil responses to multiple environmental changes.

Keywords: Dynamic model, Soil chemistry, VSD+, Deposition, Climate warming, Ecosystems

Highlights

• VSD+ dynamic soil model was applied at diverse LTER- Europe sites
• We employ data from LTER, UNECE ICP IM and ICP Forest networks
• Soil pH and BS were projected to increase under decrease in S, N deposition
• Simulations with climate warming gave more variable results
• Climate warming led to higher soil C:N at half of the sites, lower at one third

1 Introduction

Current climate warming is expected to continue in coming decades, while high European nitrogen (N) deposition may stabilize, in contrast to the clear decrease in sulphur (S) deposition (Tørseth et al. 2012, Waldner et al. 2014, Fagerli et al. 2016). The long-term impacts of N on vegetation and biodiversity in terrestrial ecosystems have been identified (Bobbink et al. 2010, Dirnböck et al. 2014, Ferretti et al. 2014) and are likely to continue unless deposition rates decline. Impacts of N on leaching water quality continue, while those of S decline with deposition (de Wit et al. 2015, Vuorenmaa et al. 2018). Climate warming and air pollution have distinctive regional patterns and their resulting impact on soil conditions and vegetation is modified by local site characteristics (Jones et al. 2004, Bertini et al. 2011, Pardo et al. 2011, Merilä et al. 2014, Jonard et al. 2015). There is increasing recognition that anthropogenic pressures and consequent environmental responses are best studied in concert in a multidisciplinary setting (e.g., De Vries et al. 2017, Mirtl et al. 2018). The direct effects of air pollution on ecosystems and habitats have been addressed through research and policy development underpinning the UNECE Convention on Long-range Transboundary Air Pollution (LRTAP Convention) (e.g., Holmberg et al. 2013, De Wit et al. 2015, Vuorenmaa et al. 2017). Informed use of science to promote sustainable development is advanced by the Intergovernmental Science-Policy Platform on Biodiversity and Ecosystem Services (IPBES) (e.g., Barnosky et al. 2012, Honrado et al. 2016). Climate change effects on ecosystems and biodiversity have been studied extensively (e.g., McMahon et al. 2011, Corlett et al. 2013, Garcia et al. 2014, He at al. 2016). Air pollution and climate change interact in numerous ways, and can mitigate effects, e.g., through increased CO_2 uptake in N-polluted forests (De Vries et al. 2006), or worsen them, e.g., through increased N_2O fluxes under N pollution, or the combined acidifying effects of N and S deposition (e.g., Forsius et al. 2005, Garmo et al. 2014). Understanding and predicting ecosystem responses to 21st century environmental change requires the capacity to simulate the combined effects of different drivers on soils, vegetation and species diversity. Combined models that include soil and species responses may provide this capacity (De Vries et al. 2010). The coupled biogeochemical and vegetation community model VSD+PROPS has been applied in the United States by McDonnell et al. (2018), who found that historical changes in N deposition had pronounced impacts on simulated HSI, a biodiversity metric (Rowe et al. 2016).

In this study we demonstrate an application of the VSD+ model (Bonten et al. 2016), with its pre-processors MetHyd and GrowUp, to 26 ecosystem study sites throughout Europe. The objectives of this work were i) to compile and report the necessary data to apply the model chain at 26 sites; ii) to evaluate the VSD+ calibration to current observations; iii) to describe future projections of soil solution pH, soil BS, C:N at 26 sites. The presented VSD+ calibrations are intended to be used for further modelling including vegetation responses. This paper provides the first phase for a demonstration of the use of a model chain that may ultimately provide input to policy analysis (Fig. 1). The sites where the models were applied represent the LTER-Europe site network (Haase et al. 2018, Mollenhauer et al. 2018), covering a wide range of environmental conditions within several distinct biomes. By including (partly co-located) sites of the ICP Forests and ICP Integrated Monitoring programmes under the LRTAP Convention (ICP Forests 2018, ICP IM 2018), we were able to make use of high quality long-term data on ecosystem response. We also used data provided by the European Monitoring and Evaluation Programme (EMEP 2018). To our knowledge, this is the first multi-site application of the VSD+ model chain at such a broad regional extent in Europe.

2 Methods

2.1 Modelling approach

We used a systems approach in applying a detailed model chain employing data and services from long-term ecological research infrastructures (Fig. 1). The single-layer soil model VSD+ (Bonten et al. 2016) accounts for processes of organic C and N turnover as well as charge and mass balances of elements, cation exchange and base cation weathering. We used VSD+ Studio (version 5.6.2, 2017) together with its accompanying pre-processors MetHyd (version 1.9.1, 2017) and GrowUp (version 1.3.2, 2017). We applied the soil dynamic model VSD+ to simulate the impacts of N and S deposition on soil solution pH (pH), soil base saturation (BS) and soil organic carbon to nitrogen ratio (C:N) at 26 sites throughout Europe (Fig. 2, Table A1). The simulations were carried out both under future climate conditions close to current climate, and with 24 regional climate scenarios, representing the two greenhouse gas concentration trajectories (RCP4.5 and RCP8.5) with twelve combinations of a modelling chain of global and regional climate models as well as bias adjustment methods (Supplementary Table A2).
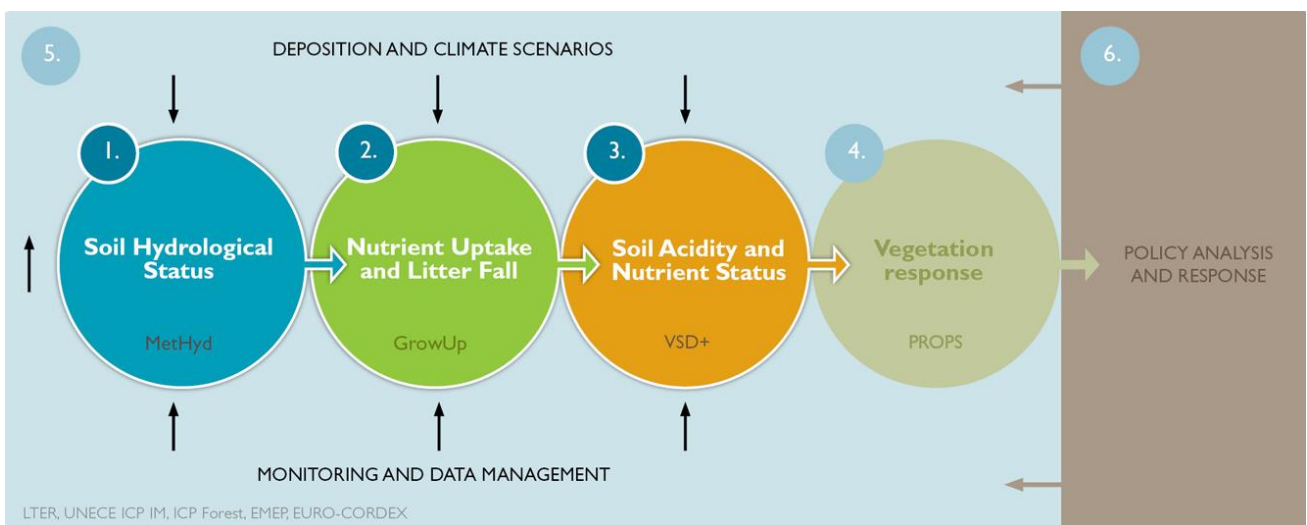
Figure 1 (and graphical abstract). Systems perspective on modelling ecosystem impacts of multiple drivers. Circles 1, 2 and 3 show the components that are the focus of this article: The model chain from MetHyd and GrowUp to the dynamic soil model VSD+ simulating soil acidity and nutrient status. The aim is to use the output of VSD+ for further modelling including vegetation responses (e.g., PROPS, circle 4). Box 5 denotes the supporting components: monitoring and data management infrastructures by

the LTER, UNECE ICP IM and ICP Forest networks, and EMEP and EURO-CORDEX-related services for providing data on current and projected deposition, and regional climate. The aim of this study is to demonstrate the use of a model chain that may ultimately provide input to policy assessment (Box 6).

2.2 Models

2.2.1 MetHyd

MetHyd is the meteo-hydrological pre-processor for hydro-meteorological data of VSD+ to calculate daily evapotranspiration, soil moisture, precipitation surplus and parameters related to N processes (Bonten et al. 2016). MetHyd reads daily data on temperature, precipitation and radiation, or, alternatively, derives daily inputs from monthly data. MetHyd input includes information on soil properties such as bulk density, the content of clay, sand and organic C. Also soil hydraulic properties (soil water content at saturation, field capacity, wilting point and at hydraulic tension of -1 bar) can be given as input to MetHyd, or derived in MetHyd from given soil properties. We used MetHyd to calculate annual values of soil moisture (*Theta, $m^3 m^{-3}$*), precipitation surplus (*percol, $m\ yr^{-1}$*), as well as soil- and temperature dependent coefficients for mineralization, nitrification and denitrification (*$rf_{\_miR}$, $rf_{\_nit}$, $rf_{\_denit}$*), used as input to VSD+ to modify the turnover rates of organic matter. Other MetHyd output variables used as VSD+ input are monthly precipitation (*Precip, mm*) and monthly average air temperature (*TempC, °C*).

2.2.2 GrowUp

GrowUp is a tool to estimate forest growth, litter fall and nutrient uptake in forest stands (Bonten et al. 2016). GrowUp reads input on (European) region, N deposition, forest growth and management (planting, thinning and clear-cut) and computes time series of uptake of N and base cations (Ca, Mg and K), and C and N in litter fall. We used GrowUp to derive annual values of uptake of N and base cations as well as the amount of C and N in litter fall returning to the soil. GrowUp calculates the uptake of Ca, Mg and K as net values (growth uptake minus litter fall), because the assumption in VSD+ is that cations are available for leaching and cation exchange immediately after root turnover or litter fall and thus only the net fluxes of these elements are needed as input to the model. The total annual litter fall flux of N, however, influences the C and N processes in VSD+, and thus N fluxes in litter fall and growth uptake are reported separately by GrowUp as input to VSD+. In GrowUp, the N content in litter fall is constrained by species-specific limit values and increases within these limits with N deposition. GrowUp uses logistic growth curves to calculate stem growth, or alternatively interpolates the annual stem growth from user-specified yield tables and management scenarios, e.g., low or no management activities in the case of unmanaged forests. The user may specify biomass expansion factors and maximum amount of leaves, or use the default values given by the model for different regions and tree species. Also, turnover rates and nutrient (N, Ca, Mg, K) contents of tree compartments have default values that can be modified by the user (Bonten et al. 2016).

2.2.3 VSD+

VSD+ (Bonten et al. 2016) is an extension of the Very Simple Dynamic (VSD) model (Posch and Reinds 2009), the latter developed to support the assessment of emissions abatements of S and N, e.g., to simulate the recovery from acidification on a European scale (Reinds et al. 2009). VSD+ is used to calculate critical loads for S and N in support of Dutch environmental policies (van Hinsberg et al. 2011, 2014, 2015, 2017). It is subject to extensive quality criteria, and relevant details on model testing,

validation and sensitivity analysis are given in Mol-Dijkstra and Reinds (2017). VSD+ has also been applied to study carbon sequestration in European forest ecosystems (De Vries et al. 2017). It is a single layer model, and its input parameters include thickness of soil layer, soil bulk density, clay content and cation exchange capacity. Options for simulating cation exchange are the Gaines-Thomas or the Gapon model, which are controlled by the values of the selectivity constants for $Al - Bc$ and $H - Bc$ exchange. Cations Ca, Mg, and K are summed as Bc, where two K^+ ions are treated as one divalent ion. In case organic acids are included in the simulations, one may use either a constant, or a pH dependent dissociation parameter (Posch and Reinds 2009). Other parameters influencing the calculations are the initial values of soil C pool, the initial C:N ratio, and the weathering rates of Ca, Mg, K and Na. VSD+ reads the results of MetHyd and GrowUp, and provides information (soil solution pH and soil C:N) that may be used as input for vegetation response modelling by , e.g., PROPS (Fig. 1). The output of VSD+ includes the soil solution concentrations of H, Al, SO_4, NO_3, NH_4, Ca, Mg, K, Na, soil base saturation (BS, exchangeable Ca, Mg and K as fractions of cation exchange capacity), and soil C and N pools (Bonten et al. 2016). A sensitivity analysis by Mol-Dijkstra and Reinds (2017) showed that the simulated soil solution pH is to a large extent determined by two parameters – the constant for the equilibrium between H^+ and Al^{3+} in the soil solution (K_Alox) and the weathering rate of Ca (Ca_we). Similarly, the exchange constant between H^+ and base cations (K_HBc) and the weathering rate of Ca (Ca_we) are the most important parameters for soil BS, whereas input of C (C_lf) and N (N_lf) in litter fall, and the uptake of N (N_upt) are important influencing factors for the simulated soil C:N ratio.

VSD+ provides input for PROPS, which is an empirical model that predicts the occurrence probabilities of plant species in response to a combination of climatic factors (temperature T, precipitation P), N deposition, soil solution pH and soil C:N ratio (Reinds et al. 2014, 2015). PROPS results allow for the calculation of several biodiversity metrics for the assessment of air pollution abatement measures (Rowe et al. 2016). PROPS has recently been applied in Austria (Dirnböck et al. 2017a) and the Eastern United States (McDonnell et al. 2018) for the assessment of combined effects of air pollution and climate change.

2.3 Data for calibration

The 26 sites of this study are part of the European network for Long Term Ecological Research (LTER Europe), the International Co-operative Programmes on Assessment and Monitoring of Air Pollution Effects on Forests (ICP Forests), and on Integrated Monitoring of Air Pollution Effects on Ecosystems (ICP IM) under the UNECE LRTAP Convention. The data used for the model applications at the sites are produced by the monitoring and data management infrastructures of these networks. The sites are forested, representing deciduous, evergreen or mixed forest, and boreal forests (taiga). They are located in Europe, in Atlantic, continental, Mediterranean, forested alpine and boreal climate regions (Figure 2, Supplementary Table A1 'Site characteristics'). The regional distribution of the sites covers the deposition gradients of air pollution in Europe, including some of the sites studied by Vuorenmaa et al. (2017). The soils at the sites include cambisols, podzols, leptosols, luvisols, histosols, regosols, stagnosols, arenosols, rendzinas, lithosols and rankers. The sites are well studied, and observations concerning past and present-day conditions that were used to set up the models and employed in the calibrations were available from previous studies (e.g., Starr et al. 1998, Larssen 2005, Ukonmaanaho et al. 2008, Bertini et al. 2011, Verstraeten et al. 2012, Ferretti et al. 2014, Zetterberg et al. 2014, Monteith et al. 2016, Sier and Monteith 2016, Dirnböck et al. 2017a, 2017b, Vuorenmaa et al. 2017). In selecting sites for the model applications, we considered data availability, both with respect to observed values of key model output variables (Supplementary Table A3 'Summary of data'), and with respect to VSD+

input parameters (Supplementary Table A4 'Input VSD+ parameter values').
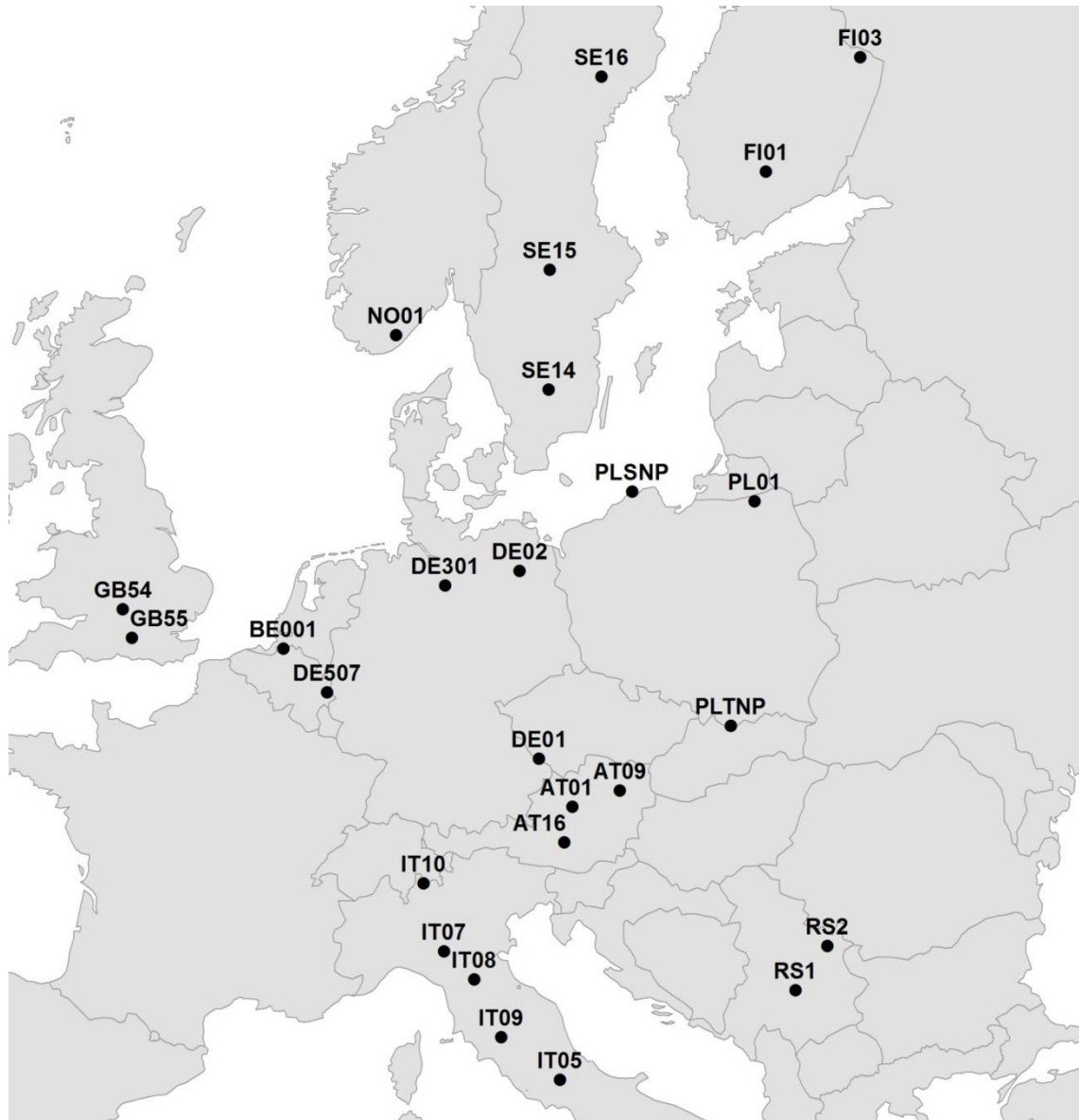
Figure 2. Location of sites where the model chain (MetHyd, GrowUp, VSD+) was applied.

MetHyd was used with site-specific monthly, or for some sites, daily observed temperature, precipitation, and sunshine or radiation data from local weather stations (e.g., Futter et al. 2011, Tørseth et al. 2012, Neyrinck et al. 2012, Aas et al. 2015). The time periods of observed current climate (Supplementary Table A5 'MetHyd input and output') covered the periods of observed soil chemistry. For example, for the Finnish sites, monthly observations of temperature (T) and precipitation (P) by the Finnish Meteorological Institute from nearby weather stations (FMI 1403 1963 – 2015 for FI01; FMI 3904 1971 – 2015 for FI03) were used. For the early simulation period, i.e., 1880 to the beginning of observed weather data, average values of the first part (until 1999) of the observations period were used, and for the late simulation period, i.e., end of observed weather data to 2100, average values of the latter part (from 2000) of the observation period were used. MetHyd was not calibrated to match observed runoff at the sites.

GrowUp was used with information on forest region, tree species and N deposition. Additional data on litter fall biomass and N concentrations were available (e.g., Fabbio and Amorini 2002, Andreassen et al. 2002, Janssens et al. 2002, Neirynck et al. 2008, Ukonmaanaho et al. 2008, Bertini et al. 2011, Kobler et al. 2015). Also, more general area and species specific yield tables were utilized; e.g., for the Finnish and

the Polish sites, information derived from the EFISCEN inventory database was used (Schelhaas et al. 2006).

For each site, observations of soil BS and C:N ratio, soil solution pH and soil solution concentrations [SO_4^{2-}], [NO_3^-], [NH_4^+], [Bc^{2+}] were available for different time periods (Neirynck et al. 2008, Wu et al. 2010, Jost et al. 2011, Köhler et al. 2011, Verstraeten et al. 2012, Ferretti et al. 2014, Zetterberg et al. 2014, Dirnböck et al. 2016, 2017a, 2017b, Timmermann et al. 2017). The periods and the number of observations used in this study are shown in Supplementary Table A3 'Summary of data'. The observations were aggregated to match the VSD+ model resolution: annual time step and one aggregated soil layer. Soil solution concentrations were aggregated over time, and soil layer specific parameters over the profile depth, as volume weighted means. The input parameter values for VSD+ are compiled in Supplementary Table A4.

2.4 Calibration

The graphical user interface of VSD+ Studio provides an automatic calibration routine, which utilizes a Bayesian approach. The probability distribution of the parameter vector is updated based on an initially assumed distribution and a dataset for verification of the model results. A Markov chain Monte Carlo method is used to perform the calibration (Reinds et al. 2008, Bonten et al. 2016). We applied the automatic calibration routine together with manual adjustment of the parameters. The final values for the calibrated parameters were chosen by taking account of both the results of the automatic calibration and visual inspection of the overall performance of the model. The following VSD+ parameters were calibrated at most sites: cation exchange (*K_AlBc, K_HBc*), the cation weathering rates (*Ca, Mg, K, Na*), the initial C pool; and 4) the initial C:N ratio. Observations of BS were used to calibrate the cation exchange parameters. Soil solution pH was used to calibrate weathering rates, as well as soil solution [Bc], when available. Observations of the C pool and the C:N ratio were used to adjust the initial values of these variables. The parameter for the dissolution of aluminium hydroxides (*K_Alox*) was also calibrated at some sites, using observations of pH and soil solution [Al^{3+}]. The calibration results were evaluated using the normalized mean absolute error (NMAE), the Pearson correlation coefficient, the coefficient of determination (RSqr) and the coefficient of efficiency (CE) evaluation metrics (Dawson et al. 2007).

2.5 Scenarios and projections

2.5.1 Deposition

Site-specific values for deposition of S and N were obtained both for past and future periods (Schöpp et al. 2003). Deposition values for 2005, 2010, 2020 and 2030 are based on the latest EMEP model version (Simpson et al. 2012), using the current legislation scenario (CLE) with revised Gothenburg Protocol emissions and a maximum feasible reduction scenario (MFR). The EMEP model provides receptor-specific deposition, to forest, semi-natural vegetation or as grid-average values at $0.50° \times 0.25°$ resolution. For the sites of this study, deposition values to forests were used. The historic deposition values are based on older EMEP- model versions (Schöpp et al. 2003).

The regional variation in deposition is reflected both in the levels of the historical peak deposition values and those of the cumulative annual deposition values for the period 1880–2100 (Fig. 3). The historical peak deposition occurred in different years at different sites. Expressed as moles of charge or equivalents (eq m^{-2} yr^{-1}), which is the relevant unit for studying the impacts on soil acidification, the peak of S

deposition was higher than peak N deposition at all sites. Only at two sites, however, are the cumulative values of S deposition higher than those of N deposition. Observed deposition fluxes of S have decreased substantially, while N deposition decreases have been less marked (Vuorenmaa et al. 2017). This levelling off of the decrease in N deposition is reflected in the N deposition projections. Simulations with VSD+ were carried out for the period 1880 to 2100 with the CLE deposition.
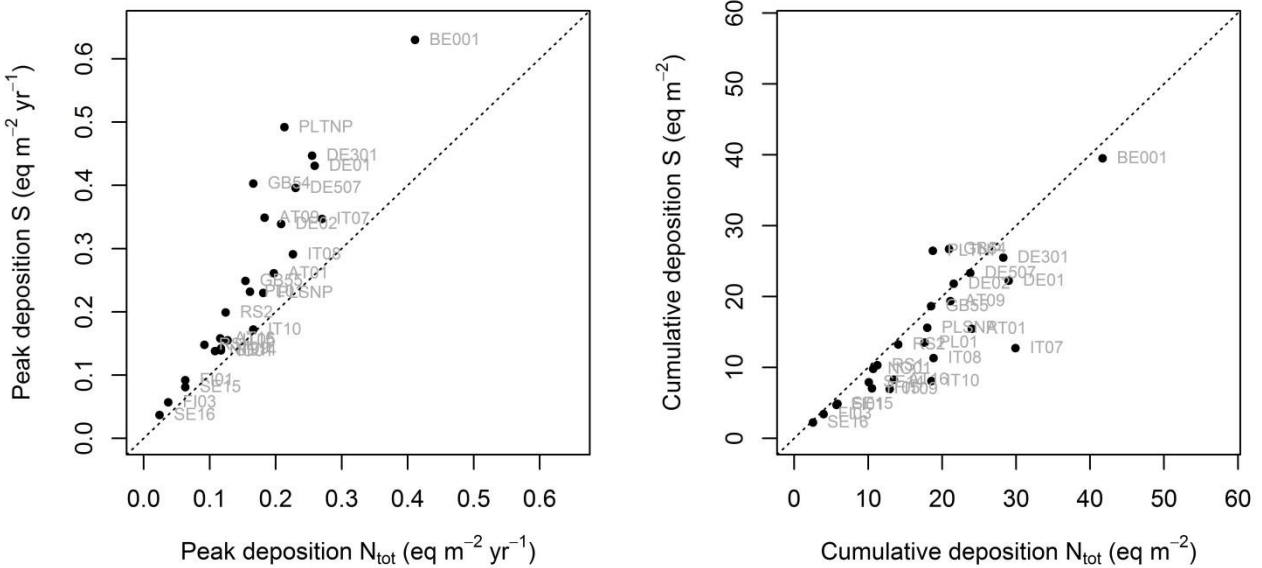
Figure 3. Historical peak deposition (left) and cumulative (1880–2100) values (right) of S deposition versus that of total N deposition onto forests at the 26 sites.

Projected future soil solution pH, soil BS and C:N were simulated for the 26 sites with the VSD+ model. The CLE scenario for S and N deposition for the period 2010 to 2100 was used as input to the simulation runs with GrowUp and VSD+.

2.5.2 Climate information

Data on future climate change used in this study were taken from an ensemble of regional climate change projections from the World Climate Research Programme's (WCRP) Coordinated Regional Downscaling Experiment (CORDEX) project, a diagnostic model inter-comparison project for CMIP6 (Giorgi et al. 2009, Gutowski et al. 2016). For this study, daily mean 2m air temperature, daily mean global radiation, and total daily precipitation regional climate model (RCM) outputs on a common 0.11° resolution pan-European grid were used. The RCM data in this study were from the EURO-CORDEX initiative, the European branch of the CORDEX project, available through the data nodes of the Earth System Grid Federation (ESGF) model data dissemination system (Cinquini et al. 2014). Within EURO-CORDEX, CMIP5 GCMs (Taylor et al. 2012) for Representative Concentration Pathways (RCPs) RCP2.6, RCP4.5, and RCP8.5 (Moss et al. 2010) have been dynamically downscaled through a coordinated multi-model, multi-physics experiment to provide high resolution, regional climate change projections (Jacob et al. 2014). Control simulations, driven by 20th century greenhouse gas concentrations (GHG), cover the time span from 1950 to 2005, from 2006 to 2100 projection simulations based on RCP GHG scenarios are available. Jacob et al. (2014) contains a basic analysis of the climate change in the EURO-CORDEX ensemble, while in evaluation studies such as Kotlarski et al. (2014), ensemble evaluation runs are compared with observations. Prein et al. (2016) investigate the added value of the 12km resolution for the reproduction of precipitation amounts and spatial patterns.

In this study, bias adjusted EURO-CORDEX RCM data, available via the ESGF data nodes were used. With process-based impact modelling, systematic biases in the RCMs as they are also inherent in the EURO-CORDEX data (Kotlarski et al. 2014) are usually corrected using a form of statistical bias adjustment; a comprehensive review on the foundations, application and limits of bias adjustment methods is given in Maraun (2016). To the EURO-CORDEX RCMs, a number of different bias adjustment schemes in combination with different calibration data sets have been applied, as indicated in Supplementary Table A2. At the time of data retrieval in April 2017, overall 69 different combinations of RCP – GCM – RCM – bias adjustment method and calibration dataset were available from the ESGF data nodes. Out of these, we selected a set of 12 combinations per RCP4.5 and RCP8.5, for which model outputs of air temperature, precipitation and radiation for both RCPs were available (see Supplementary Table A2 for an overview of datasets used). Note that only air temperature and precipitation were bias adjusted.

Our 12-member subset per RCP of the overall ensemble takes into account data availability and samples the overall spread of the climate change signals of the ensemble. Figure 4 shows, for each site, the mean climate change signals (future time span minus past time span) per model combination for the 30-year means of annual average air temperature and annual sum of precipitation for the periods 1980–2009 and 2060–2089, averaged for the 12 ensemble members per RCP (Fig. 4). The spatial distribution of changes shown in Fig. 4 resembles patterns of changes as presented, e.g., by Jacob et al. (2014, their Fig. 1 c and d). Their results indicate a temperature increase that is most pronounced in southern and (north-)eastern Europe (cf. "SE" and "FI" sites in Fig. 4) and an annual precipitation decrease in southern (c.f. "IT" sites in Fig. 4) and an increase in eastern and northern Europe. Site specific time series of 2m air temperature, global radiation and precipitation from control simulations and climate projections were extracted from the overall 24 selected ensemble members at daily resolution at the nearest neighbour grid point to the actual site location. Because the actual altitude of a site may not match with the altitude of the closest RCM grid element, the 2m air temperature was height corrected using a hypsometric lapse rate of 0.65K/100m before temporal averaging was applied.
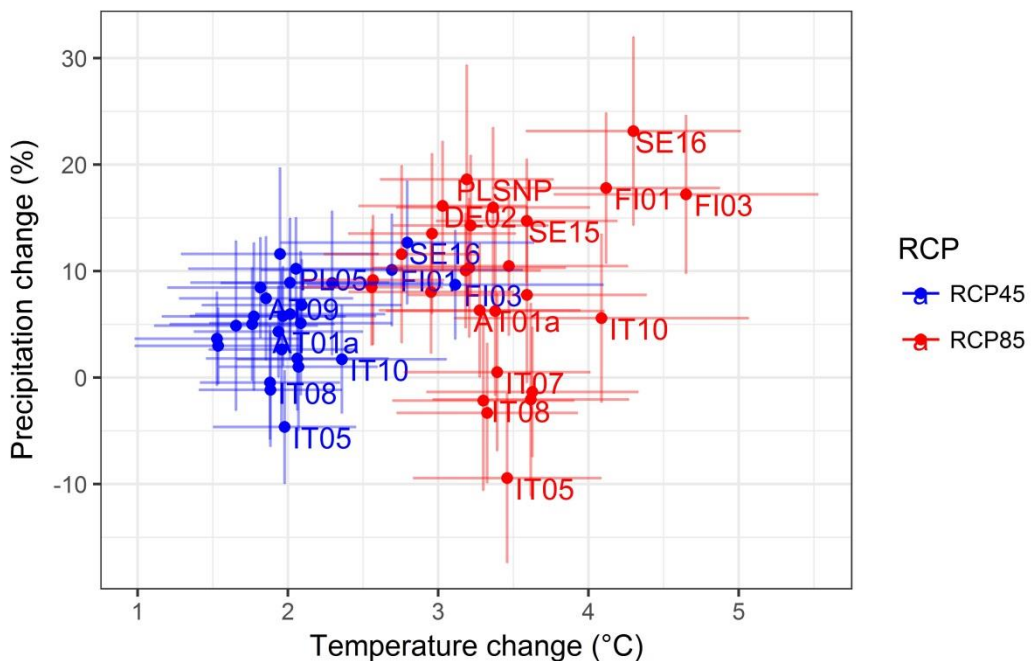
Figure 4. Scatter plot of changes in 30-yr mean values of precipitation (%) versus changes in temperature (°C) from the period 1980 – 2009 to the period 2060 – 2089. Each data point with error bars represents climate change at one site, as average over 12 ensemble members: blue for RCP4.5 and red for RCP8.5.

Error bars calculated as standard deviation of 12 ensemble members. Codes AT01 etc. refer to the sites (Fig. 2, Supplementary Table A1).

For the climate change simulations at the 26 sites MetHyd was used with monthly temperature, precipitation and radiation data according to the 12 climate change projections representing RCP4.5 and 12 projections representing RCP8.5. Simulations with the VSD+ model at the 26 sites were conducted with the 24 climate change projections according to the procedure by Dirnböck et al. (2017a), which accounts for the effects of air temperature, drought stress, and N deposition on forest growth by scaling the input to VSD+ resulting from GrowUp calculations in a manner comparable to De Vries et al. (2017). Average N and base cation uptake and C and N in litter fall derived from the observation data were scaled according to their respective climate conditions (period 1980 to 2015).

3 Results

3.1 Calibration

The observed values of soil BS, C:N and pH were all well reproduced by the calibrated models (Table 1). The observed and simulated values of BS, C:N and pH are given in Supplementary Tables A6, A7 and A8. The calibrated VSD+ parameter values are given in Supplementary Table A9. The observed and simulated values of $[NO_3^-]$, $[NH_4^+]$, $[SO_4^{2-}]$ and $[Ca+Mg+K]$ are given in Supplementary Tables A10, A11, A12 and A13. The calibration results are presented also as scatterplots (Fig. 5, Supplementary Fig. A1). Time plots for observed and modelled values of pH, $[SO_4^{2-}]$, $[NO_3^-]$, $[NH_4^+]$ and $[Ca+Mg+K]$ are given in Supplementary Figures A2, A3, A4, A5 and A6. Simulated values of BS, C:N and pH match the observations better than $[NO_3^-]$ or $[SO_4^{2-}]$. Especially for $[NH_4^+]$, the simulated values are far from the observed.

Table 1. Measures of performance

	BS	C:N	pH	$[H^+]$ (ueq L^{-1})	$[NO_3^-]$ (ueq L^{-1})	$[NH_4^+]$ (ueq L^{-1})	$[SO_4^{2-}]$ (ueq L^{-1})	$[Ca+Mg+K]$ (ueq L^{-1})
N sites	24	23	26	26	13	8	11	8
N observations	25	34	224	224	171	97	144	100
NMAE[a]	0.23	0.10	0.06	0.41	0.78	0.98	0.60	0.48
Pearson[b]	0.92	0.92	0.94	0.91	0.69	0.29	0.66	0.63
RSqr[c]	0.84	0.84	0.89	0.84	0.47	0.08	0.44	0.39
CE[d]	0.81	0.83	0.86	0.81	0.27	-0.09	0.18	0.37

[a]NMAE: Normalized mean absolute error; [b]Pearson correlation coefficient; [c]RSqr: Coefficient of determination; [d]CE: Coefficient of efficiency
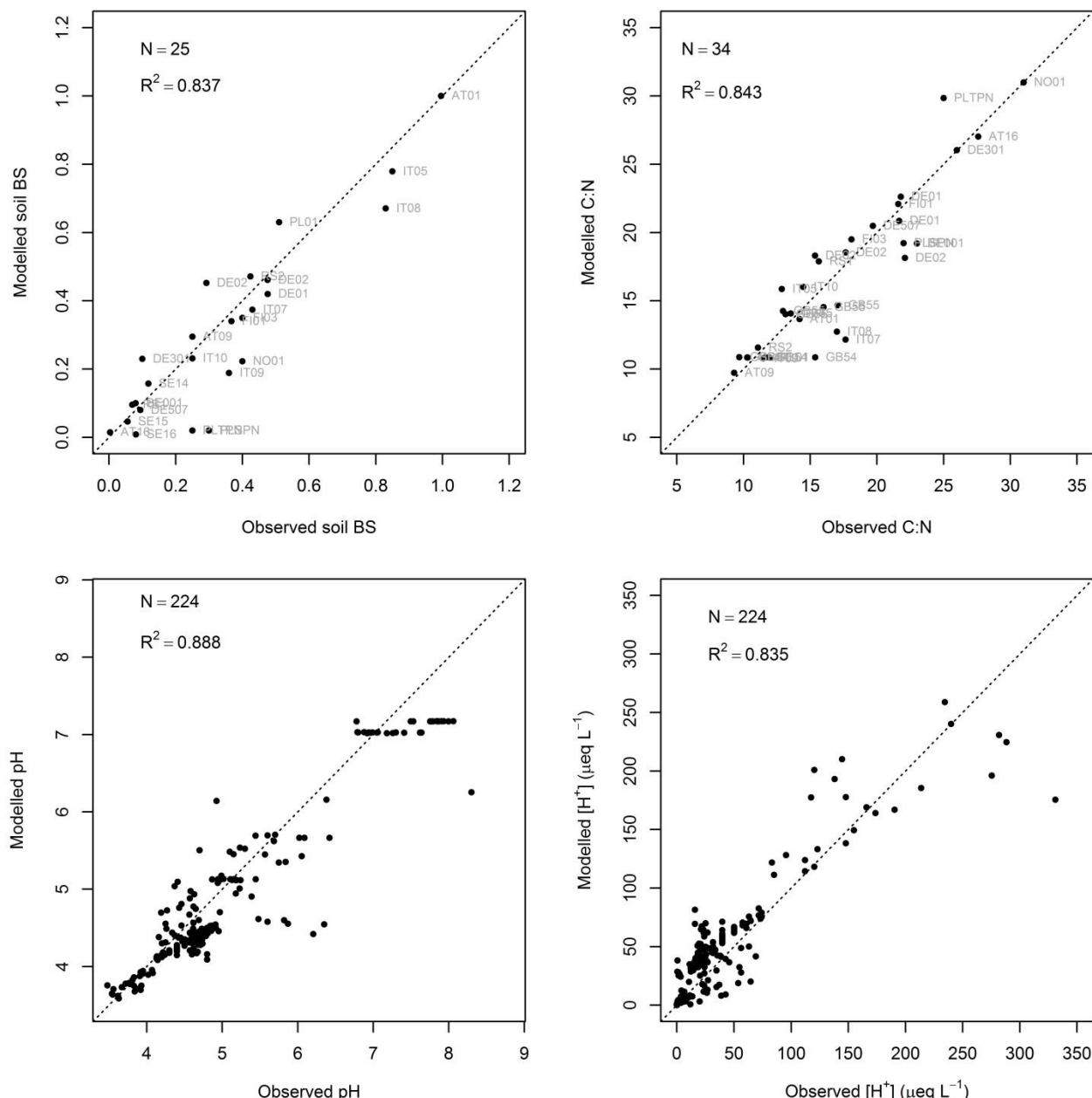
Figure 5. Modelled versus observed values of present day soil BS, C:N (g g^{-1}), soil solution pH and [H^{+}] in soil solution at the 26 sites. Dashed line represents 1:1 line. Number of observations (N) and coefficient of determination (R^2) are given in the graphs' upper left corner. Site labels are shown for BS and C:N. Data given in Supplementary Tables A6, A7 and A8. Time plots of pH are shown in Supplementary Figure A2 for those 20 sites for which more than three years of observations were used in this study.

3.2 Projected pH, BS and C:N under the CLE deposition scenario

Projected future soil conditions improved for about half of the sites. In the simulations with current climate conditions and future deposition according to the CLE scenario, soil BS and C:N for the year 2100 were more than 5% higher than for the year 2000 at 16 and 12 sites, respectively, and soil solution pH improved more than 0.02 pH units at 21 sites from 2000 to 2100 (Fig. 6). Not all the sites showed improvement, however, under the CLE deposition scenario, which represents only moderate, although realistic, deposition reductions.
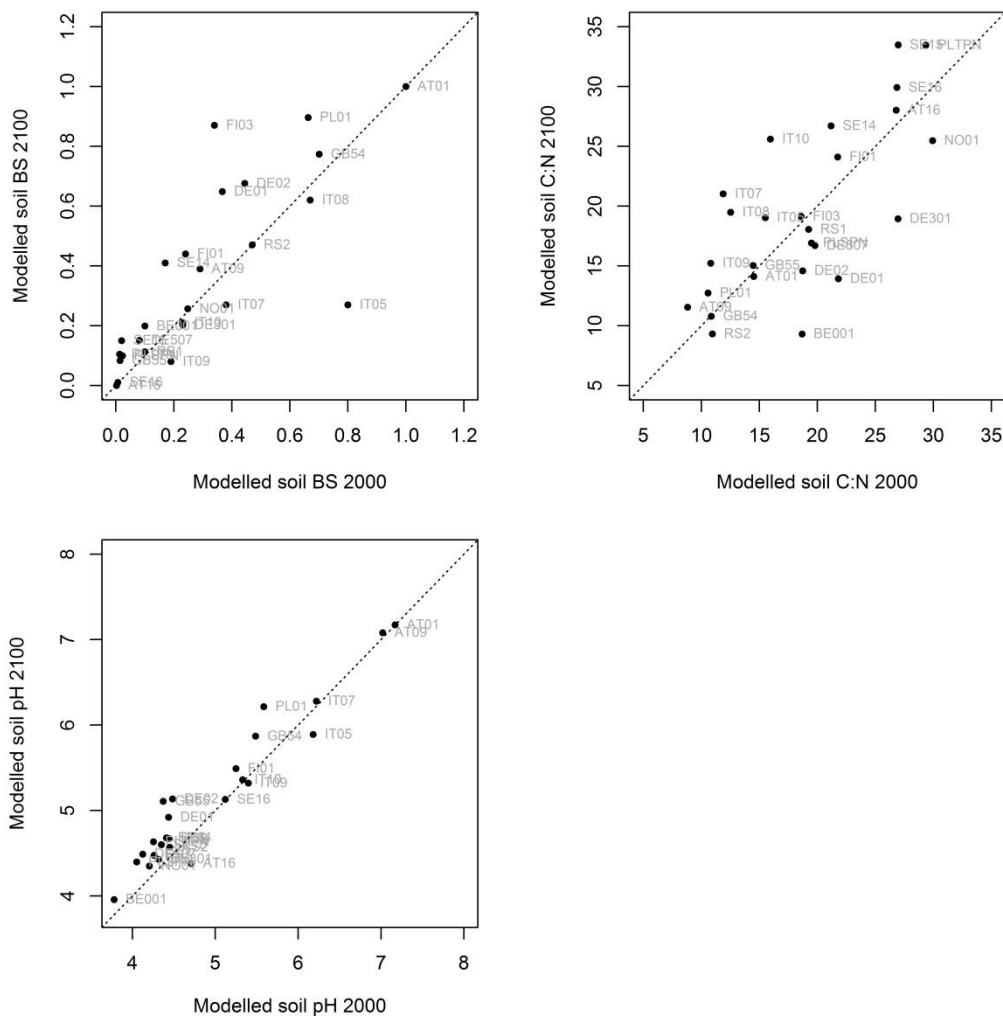
Figure 6. Modelled soil BS, C:N (g g^{-1}) and pH for the year 2100 versus modelled values for the year 2000. Simulations carried out with the CLE scenario and reference climate. Each dot represents the simulated result for one site. Dashed line represents 1:1 line.

3.3 Projected soil pH, C:N under the CLE deposition and climate change scenarios

When climate change was included in the scenario analysis, the variability of the results increased (Figs. 7, 8, 9). Climate warming clearly had an impact on soil conditions, yielding increases in simulated soil BS, C:N and pH values from the year 2000 to 2100. Especially the increase in C:N was more marked with the climate warming scenarios than with current climate.
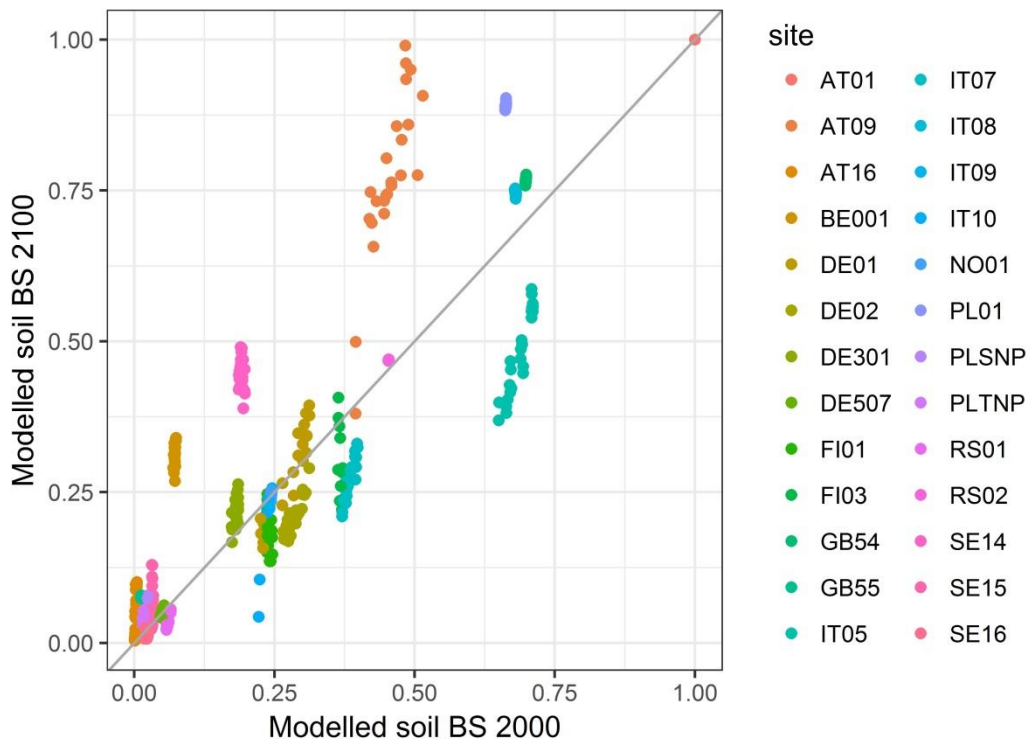
Figure 7. Modelled soil BS for 2100 versus the value for 2000 for 24 climate scenarios. Each dot represents one simulation driven by a specific downscaling model chain at a particular study site. All simulations with deposition scenario CLE. The grey line represents 1:1.
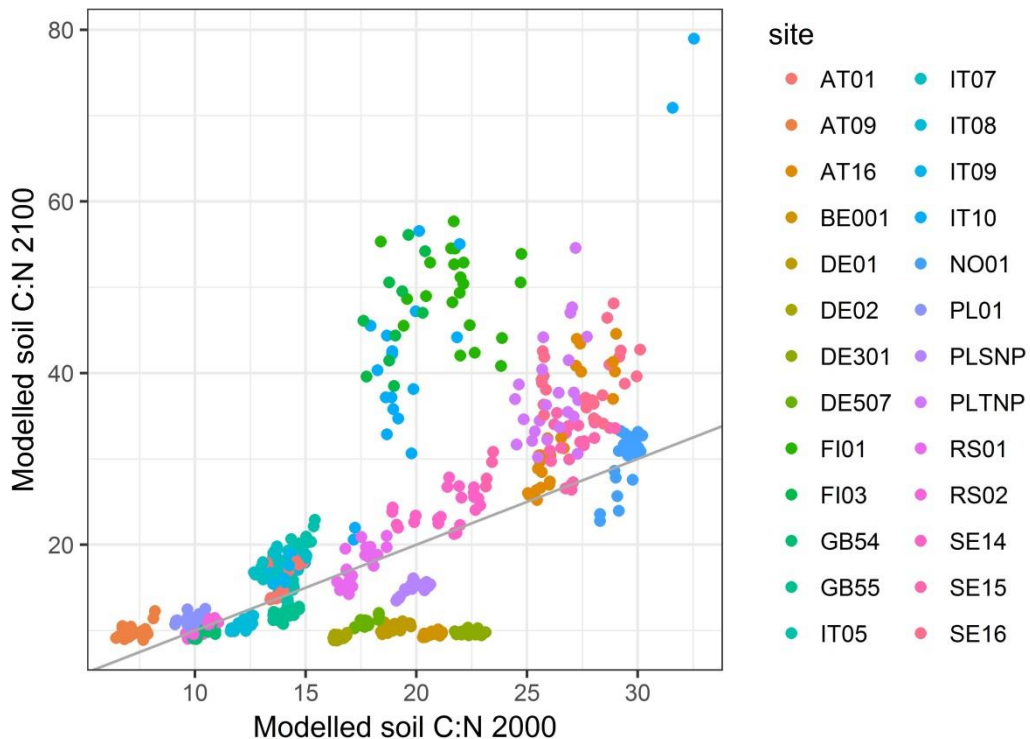
Figure 8. Modelled soil C:N for 2100 versus the value for 2000 for 24 climate scenarios. Each dot represents one simulation driven by a specific downscaling model chain at a particular study site. All simulations with deposition scenario CLE. The grey line represents 1:1.
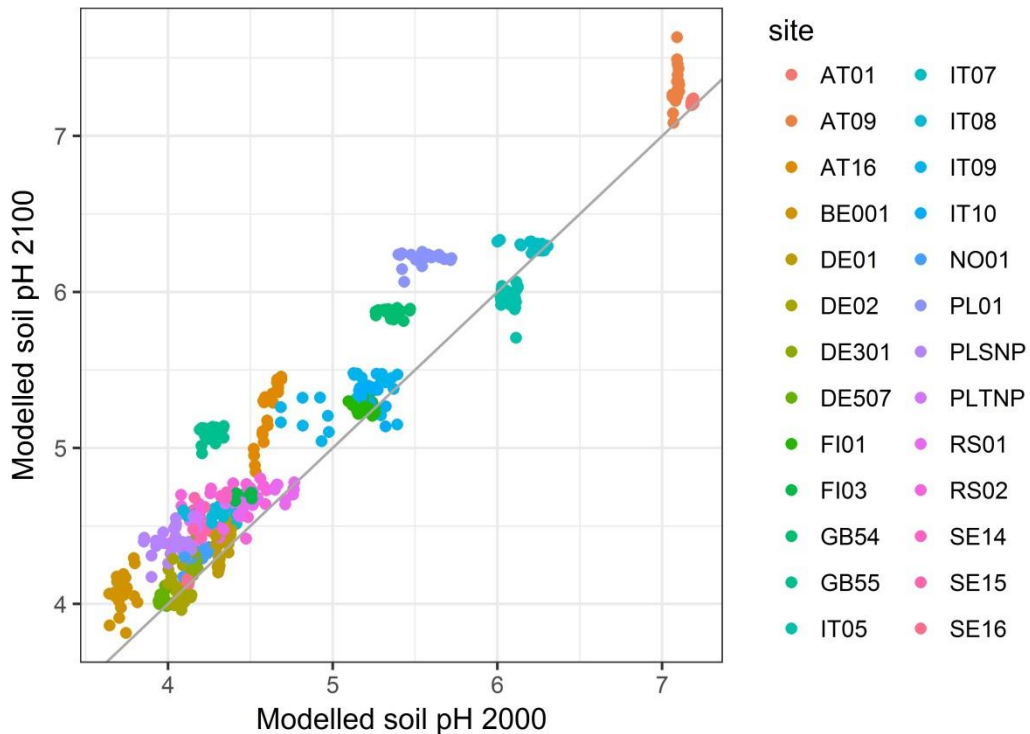
Figure 9. Modelled soil pH for 2100 versus the value for 2000 for 24 climate scenarios. Each dot represents one simulation driven by a specific downscaling model chain at a particular study site. All simulations with deposition scenario CLE. The grey line represents 1:1.

Although a number of the studied RCP8.5 climate scenarios represent pronounced warming, our set of climate scenarios include also RCP8.5 scenarios with lower projected warming, close to the warmest of the RCP4.5 scenarios (Fig. 4). This similarity is reflected in the projected soil impacts. Soil BS and C:N increased or decreased at roughly the same amount of sites per RCP (Fig. 10). Only few sites showed decreasing pH values (Fig. 10). At twelve sites soil BS values were higher in 2100 than in 2000 for all the RCP4.5 climate scenarios (Fig. 10, left). At eight sites, some of the RCP4.5 scenarios resulted in increasing BS, while other RCP4.5 scenarios gave decreasing BS values from 2000 to 2100. Only at six sites did all the RCP4.5 scenarios lead to lower BS values in 2100 than in 2000. The warmer RCP.85 scenarios yielded decreasing values only at four sites, while 22 sites for some of the scenarios. For RCP8.5, 22 sites had higher BS in 2100 than in 2000. For C:N there was a clearer division between sites: either C:N increased (fourteen or fifteen sites) or decreased (9 sites) for all the climate scenarios. Only at three (or two) sites did some climate scenarios lead to increasing and other to decreasing C:N values. Only one site had decreasing pH values for all climate scenarios (Fig. 10).

Number of sites with increasing or decreasing BS, C:N, pH
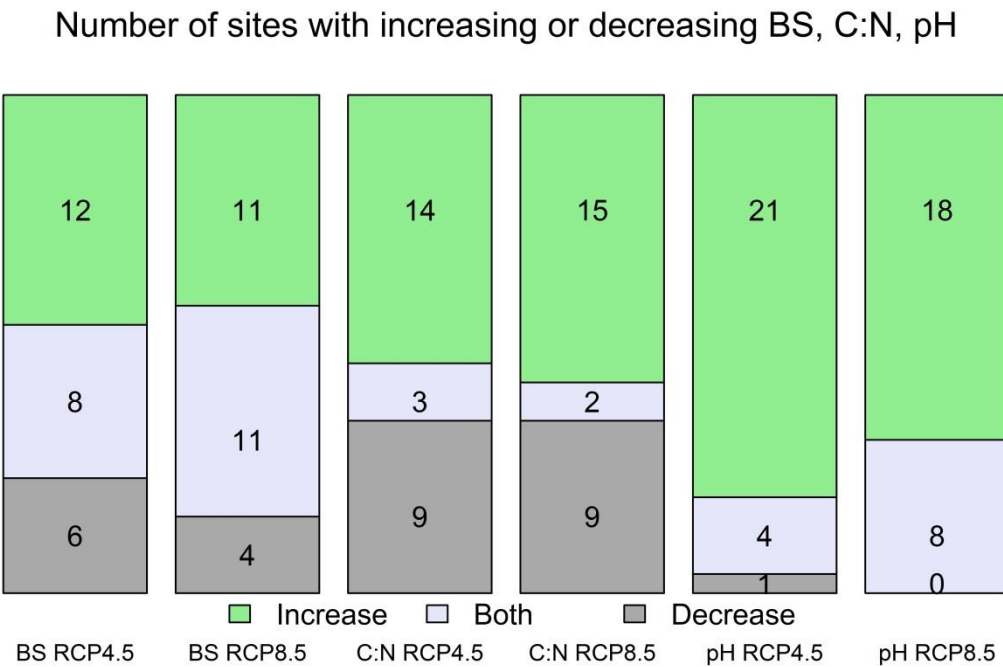
Figure 10.   Simulated change in soil variables from the year 2000 to 2100. Number of sites with only increase (top), both increase and decrease (middle) or only decrease (bottom) in BS, C:N or pH. Increase/decrease defined as BS or C:N more than 5% or pH more than 0.02 pH units higher/lower than in 2000. Simulations performed with deposition scenario CLE and twelve RCP4.5 and twelve RCP8.5 climate scenarios.

With respect to the mean change in simulated soil conditions, there were only small differences between the impacts of the RCP4.5 and RCP8.5 scenarios. At some sites the simulated mean change in BS was somewhat more pronounced with the RCP4.5 scenarios, while at other sites the RCP8.5 scenarios yielded more change. The RCP8.5 scenarios meant higher C:N at some sites but for most sites the mean changes were almost identical for RCP4.5 and RCP8.5. For simulated mean change in soil solution pH, only one site showed decrease in pH and there was hardly any difference between the two sets of climate scenarios at any of the sites.

4 Discussion and conclusions

In the VSD+ simulations roughly half of the sites showed improved soil conditions in terms of base saturation and pH under the CLE deposition scenario, without accounting for climate change (Fig. 6). The improvement corresponds with observed recovery from acidification in sensitive freshwater ecosystems (Garmo et al. 2014, DeWit et al. 2015, Vuorenmaa et al. 2017) and increased nutrient deficiency in forests (Jonard et al. 2015). Improvements (i.e., increases) in soil total C:N ratio were not evident (Fig. 6). This is to be expected, since the proportional decrease in N pollution has been less than the decrease in S pollution, and since biogeochemical responses to changes in N pollution are more varied than those to changes in S pollution. Although immobilisation of N into soil organic matter will lead to decreases in C:N ratio (Mulder et al. 2015, Cools et al. 2014), in some cases the opposite effect is seen (Jones et al. 2004), presumably due to N stimulating the production of plant litter with high C:N ratio. Site specific effects of N deposition on trends in the soil C:N ratio can further be caused by acidification controlling N

transformation in the soil (Brumme and Khanna 2008) and tree species composition (Lovett et al. 2004). In a study reporting long-term changes in input and output concentrations and fluxes at some of the same sites, Vuorenmaa et al. (2018) found a mixed response to decreasing N inputs, while S output more clearly mirrored the decreasing input.

Under climate change, soil solution pH increased for most sites (Figs. 9, 10). Also soil BS increased at many sites on the average (Figs. 7, 10). This corroborates results from others showing that warming can accelerate soil recovery from acidification, because base cation input to the soil increases with an increase in weathering and litter decomposition (Aherne et al. 2012, Gaudio et al. 2015). In some cases the climate warming scenarios resulted in pronounced increase in soil C:N (Figs 8, 10). Especially the RCP8.5 scenarios yielded high mean change in C:N, but also RCP4.5 scenarios increased C:N. At nine sites, however, soil C:N decreased for all climate scenarios. Many of these sites experience high N deposition but are also lowland sites with more severe drought effects in future. Soil water limitations can inhibit tree N uptake and SOM decomposition while N deposition accumulates in SOM causing an increase in soil N.

Our study demonstrates the need for integrated studies considering changes in both deposition and climate variables for studying long-term ecosystem impacts (Wright et al. 2006, Posch et al. 2008, Rask et al. 2014). Further, our study strongly emphasizes the importance of integrated long-term data collection of physical, chemical and biological variables for detecting the variety of impacts of changing environmental conditions on ecosystems, and for providing detailed data for dynamic model applications and scenario assessments. The large gradient in climatic conditions, deposition inputs and site conditions increase the confidence and applicability of the results obtained.

There are several sources of uncertainty involved in the evaluations of complex ecological phenomena at large spatial scales for long time periods, and the model predictions in the present study are subject to considerable uncertainty. Generally, sources of uncertainty include characteristics of the spatial data, methods for spatial interpolation, assumptions behind the scenarios, inclusion of ecosystem processes, and the temporal drivers and the process rate parameters used to derive the results (Beven 1993, Aherne et al. 2012, Mol-Dijkstra and Reinds 2017). In our study, a key source of uncertainty was the aggregation of observed soil BS and C:N to match the one-layer model, especially for sites with highly layered soil profiles. Although the overall performance of the model in reproducing observations was reasonable (Fig. 5) there were inaccuracies in reproducing key measurements at some sites. We did not calibrate MetHyd output percolation to observed runoff, which might have improved the fit of modelled concentrations. Even at sites with detailed forest and vegetation data, uncertainty was introduced by the spatial aggregation, as the estimated litter fall and growth uptake rates represented partly different locations than those for which the soil observations were aggregated. Furthermore, uncertainties in the estimates of weathering rate and the time series of C and N in litter fall and uptake of N that were used in the calibrations are reflected as uncertainties in the projections of soil solution pH, soil BS and C:N.

We found the systems approach useful in addressing the question of future impacts of climate and air pollution on soil conditions. We think this is a promising tool that helps exploring the impacts of different environmental drivers and their interactions. While impact assessments for policy support need to be done at regional and national scales, site-based modelling is helping to increase the reliability in the applied models and to quantify their uncertainties. Our aim is thus to apply the lessons learned in this work as the basis for extending the VSD+ applications to include vegetation impacts using PROPS to study deposition and climate change impacts on biodiversity metrics. This will allow impact assessments for a wider range of policies, such as EU policies on air pollution, nature and biodiversity, LRTAP Convention and IPBES.

Acknowledgements

References

Aas, W., Platt, S., Solberg, S., Yttri, K.E. 2015. Monitoring of long-range transported air pollutants in Norway, Annual Report 2014. Miljødirektoratet rapport, M-367/2015 (20/2015).

Aherne, J., Posch, M., Forsius, M., Lehtonen, A., Härkönen, K. 2012. Impacts of forest biomass removal on soil nutrient status under climate change: a catchment-based modelling study for Finland. Biogeochemistry 107, 471-488, http://dx.doi.org/10.1007/s10533-010-9569-4.

Andreassen, K., Clarke, N., Røsberg, I., Solberg, S., Aas, W. 2002. Intensive skogovervåkingsflater. Resultater fra 2001. Aktuelt fra skogforskningen 4/02:1–20.

Barnosky A.D., Hadly E.A:, Bascompte J., Berlow E.L:, Brown J.H., Fortelius M., Getz, W.M., Harte, J., Hastings, A., Marquet, P.A., Martinez, N.D., Mooers, A., Roopnarine, P., Vermeij, G., Williams, J.W., Gillespie, R., Kitzes, J., Marshall, C., Matzke, N., Mindell, D.P., Revilla, E., Smith, A.B. 2012. Approaching a state shift in Earth's biosphere. Nature 486:52–58. http://dx.doi.org/10.1038/nature11018

Bertini G., Amoriello T., Fabbio G., Piovosi M. 2011 - Forest growth and climate change. Evidences from the ICP-Forests Intensive Monitoring in Italy. iForest - Biogeosciences and Forestry 4: 262–267. doi: 10.3832/ifor0596-004

Beven, K. 1993. Prophecy, reality and uncertainty in distributed hydrological modelling. Adv. Water Resour. 16: 41–51.

Bobbink, R., Hicks, K., Galloway, J., Spranger, T., Alkemade, R., Ashmore, M., Bustamante, M., Cinderby, S., Davidson, E., Dentener, F., Emmett, B., Erisman, J.W., Fenn, M., Gilliam, F., Nordin, A., Pardo, L., De Vries, W. 2010. Global assessment of nitrogen deposition effects on terrestrial plant diversity: a synthesis. Ecological Applications 20: 30–59. DOI: 10.1890/08-1140.1

Bonten L.T.C., Reinds G.J., Posch M. 2016. A model to calculate effects of atmospheric deposition on soil acidification, eutrophication and carbon sequestration. Environmental Modelling & Software 79:75–84. http://dx.doi.org/10.1016/j.envsoft.2016.01.009

Brumme, R., Khanna, P.K. 2008. Ecological and site historical aspects of N dynamics and current N status in temperate forests. Glob Chang Biol 14:125–141. https://doi.org/10.1111/j.1365-2486.2007.01460.x

Cinquini, L., Crichton, D., Mattmann, C., Harney, J., Shipman, G., Wang, F., Ananthakrishnan, R., Miller, N., Denvil, S., Morgan, M., Pobre, Z., Bell, G.M., Doutriaux, C., Drach, R., Williams, D., Kershaw, P., Pascoe, S., Gonzalez, E., Fiore, S., Schweitzer, R. 2014. The Earth System Grid Federation: An open infrastructure for access to distributed geospatial data. Futur. Gener. Comput. Syst. 36: 400–417. http://dx.doi.org/10.1016/j.future.2013.07.002

Cools, N., Vesterdal, L., De Vos, B., Vanguelova, E., Hansen, K. 2014. Tree species is the major factor explaining C:N ratios in European forest soils. Forest Ecology and Management: 311: 3–16. http://dx.doi.org/10.1016/j.foreco.2013.06.047

Corlett, R.T., Westcott, D.A. 2013. Will plant movements keep up with climate change? Trends Ecol. Evol. 28, 482–488. https://doi.org/10.1016/j.tree.2013.04.003

Dawson, C.W., Abrahart, R.J., See, L.M. 2007. HydroTest: A web-based toolbox of evaluation metric for the standardised assessment of hydrological forecasts. Environmental Modelling & Software 22: 1034 –1052. https://doi.org/10.1016/j.envsoft.2006.06.008

De Wit, H., Hettelingh, J.-P., Harmens, H. (eds.) 2015. Trends in ecosystem and health responses to long-range transported atmospheric pollutants. ICP Waters Report 125/2015, No. 6946-2015, Norwegian Institute for Water Research, Oslo.

De Vries, W., Reinds, G.J., Gundersen, P., Sterba, H. 2006. The impact of nitrogen deposition on carbon sequestration in European forests and forest soils. Global Change Biology 12: 1151–1173.

De Vries, W., Wamelink, W., van Dobben, H., Kros, H., Reinds, G.-J., Mol-Dijkstra, J., Smart, S., Evans, C., Rowe, E., Belyazid, S., Sverdrup, H., van Hinsberg, A., Posch, M., Hettelingh, J.-P., Spranger, T., Bobbink, R. 2010. Use of dynamic soil-vegetation models to assess impacts of nitrogen deposition on plant species composition and to estimate critical loads: an overview. Ecological Applications 20: 60–79.

De Vries, W., Posch, M., Simpson, D., Reinds, G.J. 2017. Modelling long-term impacts of changes in climate, nitrogen deposition and ozone exposure on carbon sequestration of European forest ecosystems. Science of the Total Environment 605-606: 1097-1116; DOI: 10.1016/j.scitotenv.2017.06.132

Dirnböck, T., Grandin, U., Bernhardt-Römermann, M., Beudert, B., Canullo, R., Forsius, M., Grabner, M-T., Holmberg, M., Kleemola, S., Lundin, L., Mirtl, M., Neumann, M., Pompei, E., Salemaa, M., Starlinger, F., Staszewski, T., Uzięblo, A. K. 2014. Forest floor vegetation response to nitrogen deposition in Europe. Global Change Biol. 20, 429–440.

Dirnböck, T., Kobler, J., Kraus, D., Grothe, R. Kiese R. 2016. Impacts of management and climate change on nitrate leaching in a forested karst area. Journal of Environmental Management 165: 243–252.

Dirnböck T., Djukic I, Kitzler B, Kobler J, Mol-Dijkstra J.P., Posch M., Reinds G.J., Schlutow A., Starlinger F., Wamelink G.W.W. 2017a. Climate and air pollution impacts on habitat suitability of Austrian forest ecosystems. PloS ONE 12(9), e0184194. doi.org/10.1371/journal.pone.0184194.

Dirnböck, T., Foldal, C., Djukic, I., Kobler, J., Haas, E., Kiese, R., Kitzler, B. 2017b. Historic nitrogen deposition determines future climate change effects on nitrogen retention in temperate forests. Climatic Change 144(2):221–235 doi: 10.1007/s10584-017-2024-y.

EMEP 2018. Co-operative programme for monitoring and evaluation of the long-range transmissions of air pollutants in Europe. http://www.emep.int/ (accessed 20 April 2018).

Fabbio G., Amorini E. 2002 - Contribution to growth and increment analysis on the Italian CONECOFOR Level II network. Journal of Limnology, 61 (Suppl.1): 46–54. doi:https://doi.org/10.4081/jlimnol.2002.s1.46.

Fagerli, H., Tsyro, S., Denby, B.R., Olivié, D., Nyíri, A., Gauss, M., Simpson, D., Wind, P., Benedictow, A., Mortier, A., Jonson, J.E., Schultz, M., Kirkevåg, A., Valdebenito, A., Iversen, T., Seland, Ø., Aas, W., Hjellbrekke,

A.-G., Solberg, S., Rud, R.O., Tørseth, K., Yttri, K.E., Brendle, C., Mareckova, K., Pinterits, M., Schindlbacher, S., Tista, M., Ullrich, B., Wankmüller, R., Posch, M., Mona, L., Navarro, J.-C.A., Ekman, A., Hansson, H.-C., Riipinen, I., Struthers, H., Varma, V. 2016. Transboundary particulate matter, photo-oxidants, acidifying and eutrophying components. EMEP Report 1/2016, Norwegian Meteorological Institute, Oslo.

Ferretti M., Marchetto A., Arisci S., Bussotti F., Calderisi M., Carnicelli S., Cecchini G., Fabbio G., Bertini G., Matteucci G., De Cinti B., Salvati L., Pompei E. 2014 - On the tracks of Nitrogen deposition effects on temperate forests at their southern European range - an observational study from Italy. Global Change Biology 20: 3423–3438. DOI: 10.1111/gcb.12552

Forsius, M., Kleemola, S., Starr, M. 2005. Proton budgets for a network of European forested catchments: Impacts of nitrogen and sulphur deposition. Ecological Indicators 5: 73–83. https://doi.org/10.1016/j.ecolind.2004.05.001

Futter, M.N., Löfgren, S., Köhler, S.J., Lundin, L., Moldan, F., Bringmark, L., 2011. Simulating dissolved organic carbon dynamics at the Swedish integrated monitoring sites with the integrated catchments model for carbon, INCA-C. Ambio 40(8): 906–919. https://doi.org/10.1007/s13280-011-0203-z

Garcia, R.A., Cabeza, M., Rahbek, C., Araújo, M.B. 2014. Multiple Dimensions of Climate Change and Their Implications for Biodiversity. Science 344, 1247579. DOI: 10.1126/science.1247579

Garmo, Ø. A., Skjelkvåle, B.L., de Wit, H.A., Colombo, L., Curtis, C., Folster, J., Hoffmann, A., Hruška, J., Høgåsen, T., Jeffries, D.S., Keller, W.B., Krám, P., Majer, V., Monteith, D.T., Paterson, A.M., Rogora, M., Rzychon, D., Steingruber, S., Stoddard, J.L., Vuorenmaa, J., Worsztynowicz, A. 2014. Trends in surface water chemistry in acidified areas in Europe and North America from 1990 to 2008. Water Air Soil Pollut., 225:1880. DOI 10.1007/s11270-014-1880-6

Gaudio, N., Belyazid, S., Gendre, X., Mansat, A., Nicolas, M., Rizzetto, S., Sverdrup, H., Probst, A. 2015. Combined effect of atmospheric nitrogen deposition and climate change on temperate forest soil biogeochemistry: A modeling approach. Ecological Modelling 306:24–34. https://doi.org/10.1016/j.ecolmodel.2014.10.002

Giorgi, F., Jones, C., Asrar, G.R. 2009. Addressing climate information needs at the regional level: the CORDEX framework. Bulletin - World Meteorological Organization 58(3): 175–183. https://public.wmo.int/en/resources/bulletin/all-volumes

Gutowski Jr., W.J., Giorgi, F., Timbal, B., Frigon, A., Jacob, D., Kang, H.-S., Raghavan, K., Lee, B., Lennard, C., Nikulin, G., O'Rourke, E., Rixen, M., Solman, S., Stephenson, T., Tangang, F. 2016. WCRP COordinated Regional Downscaling EXperiment (CORDEX): a diagnostic MIP for CMIP6. Geosci. Model Dev. 9, 4087–4095. doi:10.5194/gmd-9-4087-2016

Haase, P., Tonkin, J.D., Stoll, S., Burkhard, B., Frenzel, M., Geijzendorffer, I.R., Häuser, C., Klotz, S., Kühn, I., McDowell, W.H,, Mirtl, M., Müller, F., Musche, M., Penner, J., Zacharias, S., Schmeller, D.S., 2018. The next generation of site-based long-term ecological monitoring: Linking essential biodiversity variables and ecosystem integrity. Sci. Total Environ. 613–614: 1376–1384. https://doi.org/10.1016/j.scitotenv.2017.08.111

He, X., He, K.S., Hyvönen, J. 2016. Will bryophytes survive in a warming world? Perspect. Plant Ecol. 19, 49–60. https://doi.org/10.1016/j.ppees.2016.02.005

Holmberg, M., Vuorenmaa, J., Posch, M., Forsius, M., Lundin, L., Kleemola, S., Augustaitis, A., Beudert, B., de Wit, H. A., Dirnböck, T., Evans, C. D., Frey, J., Grandin, U., Indriksone, I., Krám, P., Pompei, E., Schulte-Bisping, H., Srybny, A., Váňa, M. 2013. Relationship between critical load exceedances and empirical impact indicators at Integrated Monitoring sites across Europe. Ecological Indicators 24: 256–265. https://doi.org/10.1016/j.ecolind.2012.06.013

Honrado J.P., Pereira H.M., Guisan A. 2016. Fostering integration between biodiversity monitoring and modelling. Journal of Applied Ecology 53: 129 –1304. DOI:10.1111/1365-2664.12777

ICP Forests 2018. International Co-operative Programme on Assessment and Monitoring of Air Pollution Effects on Forests. http://icp-forests.net/ (accessed 20 April 2018).

ICP IM 2018. International Cooperative Programme on Integrated Monitoring of Air Pollution Effects on Ecosystems (ICP IM). http://www.syke.fi/en-US/Research__Development/Ecosystem_services/Monitoring/Integrated_Monitoring (accessed 20 April 2018).

Jacob, D., Petersen, J., Eggert, B., Alias, A., Christensen, O.B., Bouwer, L.M., Braun, A., Colette, A., Déqué, M., Georgievski, G., Georgopoulou, E., Gobiet, A., Menut, L., Nikulin, G., Haensler, A., Hempelmann, N., Jones, C., Keuler, K., Kovats, S., Kröner, N., Kotlarski, S., Kriegsmann, A., Martin, E., van Meijgaard, E., Moseley, C., Pfeifer, S., Preuschmann, S., Radermacher, C., Radtke, K., Rechid, D., Rounsevell, M., Samuelsson, P., Somot, S., Soussana, J.-F., Teichmann, C., Valentini, R., Vautard, R., Weber, B., Yiou, P. 2014. EURO-CORDEX: new high-resolution climate change projections for European impact research. Regional Environmental Change 14: 563–578. DOI:10.1007/s10113-013-0499-2

Janssens, I.A., Sampson, D.A., Curiel-Yuste, J., Carrara, A., Ceulemans, R. 2002. The carbon cost of fine root turnover in a Scots pine forest. Forest ecology and management 168: 231–240 https://doi.org/10.1016/S0378-1127(01)00755-1

Jonard, M., Fürst, A., Verstraeten, A., Thimonier, A., Timmermann, V., Potočić, N., Waldner, P., Benham, S., Hansen, K., Merilä, P., Ponette, Q., De la Cruz, A.C., Roskams, P., Nicolas, M., Croisé, L., Ingerslev, M., Matteucci, G., Decinti, B., Bascietto, M., Rautio, P. 2015. Tree mineral nutrition is deteriorating in Europe. Global Change Biology 21:418–430. doi: 10.1111/gcb.12657

Jones, M.L.M., Wallace, H.L., Norris, D., Brittain, S.A., Haria, S., Jones, R.E., Rhind, P.M., Reynolds, B.R., Emmett, B.A. 2004. Changes in vegetation and soil characteristics in coastal sand dunes along a gradient of atmospheric nitrogen deposition. Plant Biology 6(5): 598–605. DOI: 10.1055/s-2004-821004

Jost, G., Dirnböck, T., Grabner, M.-T., Mirtl, M. 2011. Nitrogen leaching of two forest ecosystems in a Karst watershed. Water, Air, & Soil Pollution 218: 633–649. DOI 10.1007/s11270-010-0674-8

Kobler, J., Jandl, R., Mirtl, M., Dirnböck, T., Schindlbacher, A. 2015. Effects of stand patchiness due to windthrow and bark beetle abatement measures on soil CO2 efflux and net ecosystem productivity of a managed temperate mountain forest. European Journal of Forest Research 134:683–692. DOI 10.1007/s10342-015-0882-2.

Köhler, S.J., Zetterberg, T., Futter, M.N., Fölster, J., Löfgren, S. 2011. Assessment of uncertainty in long-term mass balances for acidification assessments: a MAGIC model exercise. Ambio 40(8): 891–905. DOI 10.1007/s13280-011-0208-7

Kotlarski, S., Keuler, K., Christensen, O.B., Colette, A., Déqué, M., Gobiet, A., Goergen, K., Jacob, D., Lüthi, D., van Meijgaard, E., Nikulin, G., Schär, C., Teichmann, C., Vautard, R., Warrach-Sagi, K., Wulfmeyer, V. 2014. Regional climate modeling on European scales: a joint standard evaluation of the EURO-CORDEX RCM ensemble. Geosci. Model Dev. 7: 1297–1333. doi:10.5194/gmd-7-1297-2014

Larssen T. 2005. Model prognoses for future acidification recovery of surface waters in Norway using long-term monitoring data. Environ. Sci. Technol. 39:7970–7979. DOI: 10.1021/es0484247

Lovett, G.M., Weathers, K.C., Arthur, M.A., Schultz, J.C. 2004. Nitrogen cycling in a northern hardwood forest: Do species matter? Biogeochemistry 67: 289–308. https://doi.org/10.1023/B:BIOG.0000015786.65466.f5

Maraun, D. 2016. Bias Correcting Climate Change Simulations - a Critical Review. Curr. Clim. Chang. Reports 2, 211–220. doi:10.1007/s40641-016-0050-x

McDonnell, T.C., Reinds, G.J., Sullivan, T.J., Clark, C.M., Bonten, L.T.C, Mol-Dijkstra, J.P., Wamelink, G.W.W, Dovicak, M. 2018. Feasibility of coupled empirical and dynamic modeling to assess climate change and air pollution impacts on temperate forest vegetation of the eastern United States. Environ. Pollut. 234:902–914 https://doi.org/10.1016/j.envpol.2017.12.002

McMahon, S.M., Harrison, S.P., Armbruster, W.S., Bartlein, P.J., Beale, C.M., Edwards, M.E., Kattge, J., Midgley, G., Morin, X., Prentice, C.I. 2011. Trends Ecol. Evol. 26, 249–259. https://doi.org/10.1016/j.tree.2011.02.012

Merilä, P., Mustajärvi, K., Helmisaari H.-S., Hilli, S., Lindroos, A.-J., Nieminen, T.M., Nöjd, P., Rautio, P., Salemaa, M., Ukonmaanaho, L. 2014. Above- and below-ground N stocks in coniferous boreal forests in Finland:

Implications for sustainability of more intensive biomass utilization. Forest Ecology and Management 311:17–28. http://dx.doi.org/10.1016/j.foreco.2013.06.029

Mirt,l M., Borer, E.T., Djukic, I., Forsius, M., Haubold, H., Hugo, W., Jourdan, J., Lindenmayer, D., McDowell, W.H,, Muraoka, H., Orenstein, D.E., Pauw, J.C., Peterseil, J., Shibata, H., Wohner, C., Yu, X., Haase, P., 2018. Genesis, goals and achievements of Long-Term Ecological Research at the global scale: A critical review of ILTER and future directions. Sci. Total Environ. 626: 1439–1462. https://doi.org/10.1016/j.scitotenv.2017.12.001

Mulder, C., Hettelingh, J.-P., Montanarella, L., Pasimeni, M.R., Posch, M., Voigt, W., Zurlini, G. 2015. Chemical footprints of anthropogenic nitrogen deposition on recent soil C: N ratios in Europe. Biogeosciences 12: 4113–4119. https://doi.org/10.5194/bg-12-4113-2015

Mol-Dijkstra J.P., Reinds G.J. 2017. Technical documentation of the soil model VSD+. Status A. Statutory Research Tasks Unit for Nature & the Environment. Wageningen, March 2017. Available at http://edepot.wur.nl/407901 Accessed 1.6.2017

Mollenhauer, H., Kasner, M., Haase, P., Peterseil, J., Wohner, C., Frenzel, M., Mirtl, M., Schima, R., Bumberger, J., Zacharias, S., 2018. Long-term environmental monitoring infrastructures in Europe: observations, measurements, scales and socio-ecological representativeness. Sci, Total Environ, 624: 968–978.

Monteith, D., Henrys, P., Banin, L., Smith, R., Morecroft, M., Scott, T., Andrews, C., Beaumont, D., Benham, S., Bowmaker, V., Corbett, S., Dick, J., Dodd, B., Dodd, N., McKenna, C., McMillan, S., Pallett, D., Pereira, M.G., Poskitt, J., Rennie, S., Rose, R., Schafer, S., Sherrin, L., Tang, S., Turner, A., Watson, H. 2016. Trends and variability in weather and atmospheric deposition at UK Environmental Change Network sites (1993-2012). Ecological Indicators 68: 21–35. http://dx.doi.org/10.1016/j.ecolind.2016.01.061

Moss, R.H., Edmonds, J.A., Hibbard, K.A., Manning, M.R., Rose, S.K., van Vuuren, D.P., Carter, T.R., Emori, S., Kainuma, M., Kram, T., Meehl, G.A., Mitchell, J.F.B., Nakicenovic, N., Riahi, K., Smith, S.J., Stouffer, R.J., Thomson, A.M., Weyant, J.P., Wilbanks, T.J. 2010. The next generation of scenarios for climate change research and assessment. Nature 463: 747–56. doi:10.1038/nature08823

Neirynck, J., Janssens, I.A., Roskams, P., Quataert, P., Verschelde, P., Ceulemans, R. 2008. Nitrogen biogeochemistry of a mature Scots pine forest subjected to high nitrogen loads. Biogeochemistry 91: 201–222. DOI 10.1007/s10533-008-9280-x

Neirynck, J., Gielen, B., Janssens, I. A., and Ceulemans, R. 2012. Insights into ozone deposition patterns from decade-long ozone flux measurements over a mixed temperate forest. J. Environ. Monitor. 14: 1684–1695, doi:10.1039/c2em10937a.

Pardo, L. H., Fenn, M. E., Goodale, C. L., Geiser, L. H., Driscoll, C. T., Allen, E. B., Baron, J. S., Bobbink, R., Bowman, W. D., Clark, C. M., Emmett, B., Gilliam, F. S., Greaver, T. L., Hall, S. J., Lilleskov, E. A., Liu, L., Lynch, J. A., Nadelhoffer, K. J., Perakis, S. S., Robin-Abbott, M. J., Stoddard, J. L., Weathers, K. C., Dennis, R. L. 2011. Effects of nitrogen deposition and empirical nitrogen critical loads for ecoregions of the United States. Ecological Applications, 21: 3049–3082. doi:10.1890/10-2341.1

Posch, M., Aherne, J., Forsius, M., Fronzek, S., Veijalainen, N. 2008. Modelling the impacts of European emission and climate change scenarios on acid-sensitive catchments in Finland. Hydrology and Earth System Sciences 12: 449–463. https://doi.org/10.5194/hess-12-449-2008

Posch M., Reinds G.J. 2009. A very simple dynamic soil acidification model for scenario analyses and target load calculations. Environmental Modelling and Software 24:329–340. https://doi.org/10.1016/j.envsoft.2008.09.007

Posch, M., Hettelingh, J.-P., Slootweg, J., Reinds, G.J. 2014. Deriving critical loads based on plant diversity targets. In: Slootweg, J., Posch, M., Hettelingh, J.-P., Mathijssen, L. (eds.) Modelling and mapping the impacts of atmospheric deposition on plant species diversity in Europe. CCE Status Report 2014, National Institute for Public Health and the Environment, RIVM Report 2014-0075, Bilthoven, Netherlands, pp. 41–46. http://wge-cce.org/Publications/CCE_Status_Reports

Prein, A.F., Gobiet, A., Truhetz, H., Keuler, K., Goergen, K., Teichmann, C., Fox Maule, C., van Meijgaard, E., Déqué, M., Nikulin, G., Vautard, R., Colette, A., Kjellström, E., Jacob, D. 2016. Precipitation in the EURO-

CORDEX 0.11° and 0.44° simulations: high resolution, high benefits? Clim. Dyn. 46, 383–412. doi:10.1007/s00382-015-2589-y

Rask, M., Arvola, L., Forsius, M., Vuorenmaa, J. 2014. Preface to the Special Issue "Integrated Monitoring in the Valkea-Kotinen Catchment during 1990–2009: Abiotic and Biotic Responses to Changes in Air Pollution and Climate". Boreal Environment Research 19 (suppl. A): 1–3.

Reinds, G.J., Van Oijen, M., Heuvelink, G.B.M, Kros, H. 2008. Bayesian calibration of the VSD soil acidification model using European forest monitoring data. Geoderma 146:475–488. DOI: 10.1016/j.geoderma.2008.06.022

Reinds, G.J., Posch, M., Leemans, R. 2009. Modelling recovery from soil acidification in European forests under climate change. Sci Total Environ 407:5663–5673.
DOI: 10.1016/j.scitotenv.2009.07.013

Reinds, G.J., Mol-Dijkstra, J., Bonten, L., Wamelink, W., de Vries, W., Posch, M. 2014. Chapter 4. VSD+ PROPS: Recent Developments. In: Slootweg, J., Posch, M., Hettelingh, J.-P., Mathijssen, L. (eds.) Modelling and mapping the impacts of atmospheric deposition on plant species diversity in Europe. CCE Status Report 2014, National Institute for Public Health and the Environment, RIVM Report 2014-0075, Bilthoven, Netherlands, pp. 47–53. http://wge-cce.org/Publications/CCE_Status_Reports

Reinds, G.J., Mol-Dijkstra, J., Bonten, L., Wamelink, W., Hennekens, S., Goedhart, P., Posch, M. 2015. Probability of Plant Species (PROPS) model: Latest Developments. In: Slootweg, J., Posch, M., Hettelingh, J.-P. (eds) Modelling and mapping the impacts of atmospheric deposition of nitrogen and sulphur. CCE Status Report 2015, National Institute for Public Health and the Environment, RIVM Report 2015-0193, Bilthoven, Netherlands. pp. 55–62 http://wge-cce.org/Publications/CCE_Status_Reports

Rowe, E.C., Ford, A.E.S., Smart, S.M., Henrys, P.A., Ashmore, M.R., 2016. Using qualitative and quantitative methods to choose a habitat quality metric for air pollution policy evaluation. PLoS-ONE 11(8): e0161085. doi:10.1371/journal.pone.0161085.

Schelhaas, M.J., Varis, S., Schuck, A., Nabuurs, G.J. 2006. EFISCEN Inventory Database, European Forest Institute, Joensuu, Finland, http://www.efi.int/portal/virtual_library/databases/efiscen/

Schöpp, W., Posch, M., Mylona, S., Johansson, M. 2003. Long-term development of acid deposition (1880-2030) in sensitive freshwater regions in Europe. Hydrology and Earth System Sciences 7: 436–446. https://doi.org/10.5194/hess-7-436-2003

Sier, A., Monteith, D. 2016. The UK Environmental Change Network after twenty years of integrated ecosystem assessment: Key findings and future perspectives. Ecological Indicators 68:1–12. http://dx.doi.org/10.1016/j.ecolind.2016.02.008

Simpson, D., Benedictow, A., Berge, H., Bergström, R., Emberson, L.D., Fagerli, H., Flechard, C.R., Hayman, G.D., Gauss, M., Jonson, J.E., Jenkin, M.E., Nyíri, A., Richter, C., Semeena, V.S., Tsyro, S., Tuovinen, J.P., Valdebenito, Á., Wind, P. 2012. The EMEP MSC-W chemical transport model- technical description. Atmos. Chem. Phys. 12, 7825–7865. https://doi.org/10.5194/acp-12-7825-2012

Starr M., Lindroos A.-J., Tarvainen T., Tanskanen H. 1998. Weathering rates in the Hietajärvi Integrated Monitoring catchment. Boreal Environment Research 3:275–285. http://www.borenv.net/

Taylor, K.E., Stouffer, R.J., Meehl, G.A. 2012. An overview of CMIP5 and the experiment design. Bull. Am. Meteorol. Soc. doi:10.1175/BAMS-D-11-00094.1

Timmermann, V., Andreassen, K., Clarke, N., Flø, D., Magnusson, C., Nordbakken, JF., Røsberg, I., Solheim, H., Thunes, KH., Wollebæk, G., Økland, B., Aas, W. 2017. Skogens helsetilstand i Norge. Resultater fra skogskadeovervåkingen i 2016. NIBIO Rapport 3(107): 80 s. https://brage.bibsys.no/xmlui/handle/11250/2454655

Tørseth, K., Aas, W., Breivik, K., Fjæraa, A.M., Fiebig, M., Hjellbrekke, A.G., Lund Myhre, C., Solberg, S., Yttri, K.E. 2012. Introduction to the European Monitoring and Evaluation Programme (EMEP) and observed atmospheric

composition change during 1972-2009. Atmospheric Chemistry and Physics 12, 5447–5481. doi:10.5194/acp-12-5447-2012.

Ukonmaanaho L., Merilä P., Nöjd P., Nieminen T.M. 2008. Litterfall production and nutrient return to the forest floor in Scots pine and Norway spruce stands in Finland. Boreal Environment Research 13 (suppl. B): 67–91. http://www.borenv.net/

Van Hinsberg, A., Reinds G.J., Mol, J. 2011. Netherlands contribution to NFC reports. In: Posch, M., Slootweg, J., Hettelingh, J.-P. (eds.) Modelling critical thresholds and temporal changes of geochemistry and vegetation diversity. CCE Status Report 2011, National Institute for Public Health and the Environment, RIVM Report 68035903, Bilthoven, Netherlands. pp. 147–154. http://wge-cce.org/Publications/CCE_Status_Reports

Van Hinsberg, A., Reinds G.J., Mol, J. 2014. Netherlands contribution to NFC reports. In: Slootweg, J., Posch, M., Hettelingh, J.-P., Mathijssen, L. (eds.) Modelling and Mapping the impacts of atmospheric deposition on plant species diversity in Europe. CCE Status Report 2014, Coordination Centre for Effects, National Institute for Public Health and the Environment, RIVM Report 2014-0075, Bilthoven, Netherlands. pp. 147–154. http://wge-cce.org/Publications/CCE_Status_Reports

Van Hinsberg, A., Reinds G.J., Mol, J. 2015. Netherlands contribution to NFC reports. In: Slootweg, J., Posch, M., Hettelingh, J.-P. (eds.) Modelling and mapping the impacts of atmospheric deposition on nitrogen and sulphur. CCE Status Report 2015, National Institute for Public Health and the Environment, RIVM Report 2015-0193, Bilthoven, Netherlands. pp. 147–154. http://wge-cce.org/Publications/CCE_Status_Reports

Van Hinsberg, A., Reinds G.J., Mol, J. 2017. Netherlands contribution to NFC reports. In: Hettelingh, J.-P., Posch, M., Slootweg, J. (eds.) European critical loads: database, biodiversity and ecosystems at risk. CCE Final Report 2017, National Institute for Public Health and the Environment, RIVM Report 2017-0155, Bilthoven, Netherlands. pp. 147–154. http://wge-cce.org/Publications/CCE_Status_Reports

Verstraeten, A., Neirynck, J., Genouw, G., Cools, N., Roskams, P., Hens, M., 2012. Impact of declining atmospheric deposition on forest soil solution chemistry in Flanders, Belgium. Atmospheric Environment, 62: 20–63. http://dx.doi.org/10.1016/j.atmosenv.2012.08.017

Vuorenmaa, J., Augustaitis, A., Beudert, B., Clarke, N., de Wit, H.A., Dirnböck, T., Frey, J., Forsius, M., Indriksone, I., Kleemola, S., Kobler, J., Krám, P., Lindroos, A.-J., Lundin, L., Ruoho-Airola, T., Ukonmaanaho, L., Váňa, M. 2017. Long-term sulphate and inorganic nitrogen mass balance budgets in European ICP Integrated Monitoring catchments (1990–2012). Ecol. Ind. 76: 15–29. http://dx.doi.org/10.1016/j.ecolind.2016.12.040

Vuorenmaa J., Forsius M., Augustaitis A., Beudert B., Bochenek W., Clarke N., de Wit, H.A., Dirnböck, T., Frey, J., Hakola, H., Kleemola, S., Kobler, J., Krám, P., Lindroos, A.-J., Lundin, L., Löfgren, S., Marchetto, A., Pecka, T., Schulte-Bisping, H., Skotak, K., Srybny, A., Szpikowski, J., Ukonmaanaho, L., Vàna, M., Åkerblom, S., Forsius, M. 2018. Long-term changes (1990-2015) in the atmospheric deposition and runoff water chemistry of sulphate, inorganic nitrogen and acidity for forested catchments in Europe in relation to changes in emissions and hydrometeorological conditions. Sci. Total Environ. 625:1129–1145. DOI: 10.1016/j.scitotenv.2017.12.245

Waldner, P., Marchetto, A., Thimonier, A., Schmitt, M., Rogora, M., Granke, O., Mues, V., Hansen, K., Pihl-Karlsson, G., Žlindra, D., Clarke, N., Verstraeten, A., Lazdins, A., Schimming, C., Iacoban, C., Lindroos, A.-J., Vanguelova, E., Benham, S., Meesenburg, H., Nicolas, M., Kowalska, A., Apuhtin, V., Napa, U., Lachmanová, Z., Kristoefel, F., Bleeker, A., Ingerslev, M., Vesterdal, L., Molina, J., Fischer, U., Seidling, W., Jonard, M., O'Dea, P., Johnson, J., Fischer, R., Lorenz, M., 2014. Detection of temporal trends in atmospheric deposition of inorganic nitrogen and sulphate to forests in Europe. Atmos. Environ. 95, 363–374. http://dx.doi.org/10.1016/j.atmosenv.2014.06.054

Wright, R.F., Aherne, J., Bishop, K., Camarero, L., Cosby, B.J., Erlandsson, M., Evans, C.D., Forsius, M., Hardekopf, D., Helliwell, R., Hruska, J., Jenkins, A., Moldan, F., Posch, M., Rogora, M. 2006. Modelling the effect of climate change on recovery of acidified freshwaters: relative sensitivity of individual processes in the MAGIC model. Science of the Total Environment 365: 154–166. doi:10.1016/j.scitotenv.2006.02.042

Wu, Y., Clarke, N., Mulder, J. 2010. Dissolved Organic Nitrogen Concentrations and Ratios of Dissolved Organic Carbon to Dissolved Organic Nitrogen in Throughfall and Soil Waters in Norway Spruce and Scots Pine Forest Stands Throughout Norway. Water Air Soil Pollution 210: 171–186. https://doi.org/10.1007/s11270-009-0239-x

Zetterberg, T., Köhler, S. J., Löfgren, S. 2014. Sensitivity analyses of MAGIC modelled predictions of future impacts of whole-tree harvest on soil calcium supply and stream acid neutralizing capacity. Science of the Total Environment 494: 187–201. http://dx.doi.org/10.1016/j.scitotenv.2014.06.114

Supplementary Tables STOTEN-27089
Modelling study of soil C, N and pH response to air pollution and climate change using European LTER site observations

Holmberg, M., Aherne, J., Austnes, K., Beloica, J., De Marco, A., Dirnböck, T., Fornasier, M.F., Goergen, K., Futter, M., Lindroos, A.-J., Krám, P., Neirynck, J., Nieminen, T.M., Pecka, T., Posch, M., Pröll, G., Rowe, E.C., Scheuschner, T., Schlutow, A., Valinia, S., Forsius, M.

Table of contents:

Supplementary Table A1. Site characteristics of 26 sites for which the VSD+ model was applied

Country	Site Code for VSD+ study	Site	Longitude (decimal coord.)	Latitude (decimal coord.)	Altitude (m a.s.l)	Networks[1]	ILTER Biome	Biogeographic region	Soils
Austria	AT01	Zöbelboden IP1	14.44	47.84	895	IM, LTER	Mixed forest	Alpine	Chromic Cambisols and hydromorphic Stagnosols
Austria	AT09	Klausen-Leopoldsdorf	16.05	48.12	510	FO, LTER	Deciduous Forest	Alpine	Endostagnic Endoskeletic Luvisol
Austria	AT16	Murau	14.11	47.06	1540	FO, LTER	Evergreen Forest	Subalpine	Hyperdystric Endoskeletic Cambisol
Belgium	BE001	Brasschaat	4.52	51.31	14	FO, LTER	Evergreen Forest	Atlantic	Moderately wet and sandy Arenosol with distinct horizons of humus and iron, forest floor mor-moder type
Germany	DE01	Forellenbach	13.42	48.94	894	IM, LTER	Deciduous Forest	Continental	Dystric Cambisol
Germany	DE02	Neuglobsow	13.03	53.13	65	IM	Mixed forest	Continental	Eutric Cambisol
Germany	DE301	Lüss	10.28	52.84	125	FO, LTER	Deciduous Forest	Atlantic	Albic Rustic Podzol
Germany	DE507	Monschau	6.15	50.4	445	FO, LTER	Deciduous Forest	Atlantic	Dystric Cambisol
Finland	FI01	Valkea-Kotinen	25.06	61.24	165	IM, FO, LTER	Taiga	Boreal	Cambic Podzol
Finland	FI03	Hietajärvi	30.68	63.15	170	IM, FO	Taiga	Boreal	Haplic Podzol
United Kingdom	GB54	Wytham	-1.33	51.77	138	LTER	Deciduous	Atlantic	Eutric Vertic Stagnosols
United Kingdom	GB55	Alice Holt	-0.85	51.17	125	IM, FO, LTER	Deciduous	Atlantic	Eutric Vertic Stagnosols
Italy	IT05	Selva Piana	13.59	41.85	1500	IM, FO, LTER	Deciduous Forest	Alpine	Orthic Rendzinas
Italy	IT07	Carrega	10.2	44.73	200	IM, FO	Deciduous Forest	Continental	Plano-Gleyic Luvisols
Italy	IT08	Brasimone	11.12	44.11	975	IM, FO	Deciduous Forest	Continental	Calcaric Regosols
Italy	IT09	Monte Rufeno	11.9	42.83	690	IM, FO, LTER	Deciduous Forest	Mediterranean	Calcaric Regosols
Italy	IT10	Val Masino	9.55	46.24	1190	IM, FO, LTER	Evergreen Forest	Alpine	Dystrict Lithosols
Norway	NO01	Birkenes	8.25	58.38	190	IM, FO, LTER	Taiga	Boreal	Podzol and Cambisol
Poland	PL01	Puszcza Borecka	22.05	54.12	170	IM	Deciduous forest	Continental	Luvisol

Poland	PLSNP	Słowiński National Park	17.47	54.7	15	FO, LTER	Evergreen Forest	Continental	Histo-Humic Gleysol
Poland	PLTNP	Tatrzański National Park	19.99	49.27	970	LTER	Evergreen Forest	Alpine	Calcaric Lithosol
Serbia	RS1	Kopaonik	20.81	43.29	1700	FO, LTER	Mixed forest	Continental	Cambic Podzol, Humic Cambisol
Serbia	RS2	Crni vrh	21.98	44.13	940	FO, LTER	Deciduous forest	Continental	Dystric Cambisol
Sweden	SE14	Aneboda	14.53	57.12	230	IM, LTER	Taiga	Boreonemoral	Podzol
Sweden	SE15	Kindla	14.9	59.75	345	IM, LTER	Taiga	Boreal	Podzol
Sweden	SE16	Gammtratten	18.1	63.86	425	IM, LTER	Taiga	Boreal	Podzol and Histosol

[1] Networks:
FO (UNECE ICP Forests, International Co-operative Programme on Assessment and Monitoring of Air Pollution Effects on Forests under the United Nation's Economic Commission for Europe);
IM (UNECE ICP IM, International Co-operative Programme on Assessment and Monitoring of Air Pollution Effects on Ecosystems under the United Nation's Economic Commission for Europe);
LTER (LTER Europe, International Long Term Ecological Research regional network for Europe)

Supplementary Table A2. List of combinations of RCP – GCM – RCM -bias adjustment and reference data in the 24 ensemble members used in the study. For each model combination air temperature and precipitation are available bias adjusted; global radiation is based on the same RCP – GCM – RCM combination, albeit not bias adjusted. The naming is based on the official CORDEX data protocol data reference syntax controlled vocabulary. Using these identifiers data can be found on any ESGF data node (e.g., https://esgf-node.ipsl.upmc.fr/projects/esgf-ipsl/). The table is sorted according to driving GCM and CMIP5 experiment name. Meaning of the bias adjustment methods: DBS45, distribution based scaling from Swedish Meteorological and Hydrological Institute (SMHI) (Yang et al., 2010); CDFT21, cumulative distribution function from Institut Pierre Simon Laplace (IPSL) (Vrac et al., 2016). Meaning of the bias adjustment calibration datasets: MESAN, regional reanalysis (from EU FP7 EURO4M project) from SMHI (Landelius et al., 2016); WFDEI, WATCH forcing data methodology applied to ERA-Interim (from FP6 WATCH project) (Weedon et al., 2014). Overall six different bias adjustment schemes and three different calibration datasets have been applied to the CORDEX RCMs by different institutions.

Combination identifier (Fig. 4)	GCM model name, institute identifier and model identifier	CMIP5 experiment name (ensemble member not mentioned)	Institution which ran RCM	RCM model name and version	RCM model run version	Institution that did bias adjustment	Bias adjustment method	Bias adjustment calibration dataset	Time span over which bias adjustment calibrated
A	CNRM-CERFACS-CNRM-CM5	RCP45 / RCP85	CLMcom	CCLM4-8-17	v1	SMHI	DBS45	MESAN	1989-2010
B	CNRM-CERFACS-CNRM-CM5	RCP45 / RCP85	CNRM	ARPEGE51	v1	IPSL	CDFT21	WFDEI	1979-2005
C	CNRM-CERFACS-CNRM-CM5	RCP45 / RCP85	SMHI	RCA4	v1	IPSL	CDFT21	WFDEI	1979-2005
D	ICHEC-EC-EARTH	RCP45 / RCP85	KNMI	RACMO22E	v1	IPSL	CDFT21	WFDEI	1979-2005
E	IPSL-IPSL-CM5A-MR	RCP45 / RCP85	IPSL-INERIS	WRF331F	v1	IPSL	CDFT21	WFDEI	1979-2005
F	IPSL-IPSL-CM5A-MR	RCP45 / RCP85	SMHI	RCA4	v1	IPSL	CDFT21	WFDEI	1979-2005
G	MOHC-HadGEM2-ES	RCP45 / RCP85	CLMcom	CCLM4-8-17	v1	SMHI	DBS45	MESAN	1989-2010
H	MOHC-HadGEM2-ES	RCP45 / RCP85	KNMI	RACMO22E	v2	SMHI	DBS45	MESAN	1989-2010
I	MOHC-HadGEM2-ES	RCP45 / RCP85	SMHI	RCA4	v1	IPSL	CDFT21	WFDEI	1979-2005
J	MPI-M-MPI-ESM-LR	RCP45 / RCP85	CLMcom	CCLM4-8-17	v1	SMHI	DBS45	MESAN	1989-2010
K	MPI-M-MPI-ESM-LR	RCP45 / RCP85	MPI-CSC	REMO2009	v1	SMHI	DBS45	MESAN	1989-2010
L	MPI-M-MPI-ESM-LR	RCP45 / RCP85	SMHI	RCA4	v1	IPSL	CDFT22	WFDEI	1979-2005

Landelius, T., Dahlgren, P., Gollvik, S., Jansson, A., Olsson, E., 2016. A high-resolution regional reanalysis for Europe. Part 2: 2D analysis of surface temperature, precipitation and wind. Q. J. R. Meteorol. Soc. 142, 2132–2142. doi:10.1002/qj.2813

Vrac, M., Noël, T., Vautard, R., 2016. Bias correction of precipitation through Singularity Stochastic Removal: Because occurrences matter. J. Geophys. Res. Atmos. 121, 5237–5258. doi:10.1002/2015JD024511

Weedon, G.P., Balsamo, G., Bellouin, N., Gomes, S., Best, M.J., Viterbo, P., 2014. The WFDEI meteorological forcing data set: WATCH Forcing Data methodology applied to ERA-Interim reanalysis data. Water Resour. Res. 50, 7505–7514. doi:10.1002/2014WR015638

Yang, W., Andréasson, J., Phil Graham, L., Olsson, J., Rosberg, J., Wetterhall, F., 2010. Distribution-based scaling to improve usability of regional climate model projections for hydrological climate change impacts studies. Hydrol. Res. 41, 211. doi:10.2166/nh.2010.004

Supplementary Table A3. Summary of data used in calibration of VSD+. Number and year of observations.

Site	BS N	years	C:N N	years	pH N	years	[SO$_4$] N	years	[NO$_3$] N	years	[NH$_4$] N	years	[Bc] [1] N	years
AT01	1	2004	1	2004	15	1998 - 2012	15	1998 - 2012	15	1998 - 2012	-	-	-	-
AT09	1	2008	1	2008	15	1998 - 2012	15	1998 - 2012	15	1998 - 2012	-	-	-	-
AT16	1	2008	1	2008	14	1998 - 2011	14	1998 - 2011	14	1998 - 2011	-	-	-	-
BE001	1	2004	1	2004	24	1992 - 2015	24	1992 - 2015	24	1992 - 2015	-	-	24	1992 - 2015
DE01	1	2010	2	1990; 2011	22	1991 -2012	-	-	-	-	-	-	-	-
DE02	2	2005; 2010	3	2005 - 2013	1	2005	-	-	-	-	-	-	-	-
DE301	1	2007	1	2007	6	1996 - 2001	-	-	-	-	-	-	-	-
DE507	1	2007	1	2007	6	1996 - 2001	-	-	-	-	-	-	-	-
FI01	1	1988	1	2006	5	2002 - 2006	3	2002 - 2006	3	2002 - 2006	3	2002 - 2006	3	2002 - 2006
FI03	1	1988	1	2006	5	2002 - 2006	5	2002 - 2006	5	2002 - 2006	5	2002 - 2006	5	2002 - 2006
GB54	-	-	5	1993 - 2013	5	1993 - 2013	-	-	-	-	-	-	-	-
GB55	-	-	5	1994 - 2014	5	1994 - 2014	-	-	-	-	-	-	-	-
IT05	1	2006	1	2006	1	1999	-	-	-	-	-	-	-	-
IT07	1	2006	1	2006	1	2006	-	-	-	-	-	-	-	-
IT08	1	2006	1	2006	1	2006	-	-	-	-	-	-	-	-
IT09	1	2006	1	2006	2	2006 - 2008	-	-	-	-	-	-	-	-
IT10	1	2006	1	2006	1	2006	-	-	-	-	-	-	-	-
NO01	1	1991	1	1991	22	1993 - 2014	-	-	22	1993 - 2014	22	1993 - 2014	-	-
PL01	1	1985	1	2004	5	1995 - 2013	-	-	5	1995 - 2013	-	-	-	-
PLTPN	1	2004	1	2004	3	1998 - 2012	-	-	-	-	-	-	-	-
PLSPN	1	2004	1	2004	3	1998 - 2012	-	-	-	-	-	-	-	-
RS1	1	2010	1	2010	1	2010	6	2011 - 2016	6	2011 - 2016	6	2011 - 2016	5	2012 - 2016
RS2	1	2013	1	2013	1	2013	9	2014 - 2016	9	2014 - 2016	9	2014 - 2016	9	2014 - 2016
SE14	1	2007	-	-	20	1994 - 2013	22	1994 - 2015	22	1994 - 2015	22	1994 - 2015	22	1994 - 2015
SE15	1	2007	-	-	20	1994 - 2013	22	1994 - 2915	22	1994 - 2915	22	1994 – 2915	22	1994 - 2915
SE16	1	2007	-	-	13	2000 - 2013	15	2000 - 2015	15	2000 - 2015	15	2000 - 2015	15	2000 - 2015

[1] [Bc^{2+}] is the sum of Ca, Mg and K, where two K$^+$ ions are treated as one divalent ion.

Supplementary Table A4. Input VSD+ parameter values.

Site	Thickness (m)	Bulk density (g cm^{-3})	CO$_2$ pressure	Calcium in parent material (1)	Clay content (%)	CEC (meq kg^{-1})	Exchange model (2)	Organic acids model (3)	Parameters organic acids model (4)	Concentration of organic acids (mol m^{-3})
AT01	0.5	0.611	18	0.5	38.0	511.2	-	Mono-protic organic acid	4.5	0.320
AT09	0.59	1.099	19.2		43.0	68.5	Gaines-Thomas	Mono-protic organic acid	4.5	0.050
AT16	0.45	0.671	15.3		21.0	74.6	Gaines-Thomas	Mono-protic organic acid	2.8	0.066
BE001	0.8	1.450	23		5.0	15.0	Gaines-Thomas	Oliver model	0.96; 0.9; 0.039	0.062
DE01	0.7	1.410	15		3.0	36.2	Gapon	Mono-protic organic acid	4.5	0.500
DE02	0.8	1.300	15		2.3	30.6	Gapon	Mono-protic organic acid	0	0.250
DE301	0.8	1.293	15		5.5	70.3	Gapon	Mono-protic organic acid	0	0.500
DE507	0.8	1.196	15		27.2	93.0	Gapon	Mono-protic organic acid	0	0.500
FI01	0.435	0.954	33		5.3	46.8	Gaines-Thomas	Oliver model	0.96; 0.9; 0.039	0.004
FI03	0.435	1.342	33		1.0	6.8	Gaines-Thomas	Oliver model	0.96; 0.9; 0.039	0.004
GB54	0.4	1.149	33		80.0	222.2	Gaines-Thomas	Oliver model	0.96; 0.9; 0.039	0.004
GB55	0.4	1.149	33		60.0	279.7	Gaines-Thomas	Oliver model	0.96; 0.9; 0.039	0.004
IT05	0.2	0.871	19.5		26.0	166.5	Gaines-Thomas	Oliver model	0.96; 0.9; 0.039	0.010
IT07	0.6	1.063	24.3		21.0	125.2	Gaines-Thomas	Oliver model	0.96; 0.9; 0.039	0.010
IT08	0.42	1.269	22.7		30.0	123.8	Gaines-Thomas	Oliver model	0.96; 0.9; 0.039	0.010
IT09	0.53	1.183	24		25.0	178.8	Gaines-Thomas	Oliver model	0.96; 0.9; 0.039	0.010
IT10	0.53	0.905	20.2		15.0	197.5	Gaines-Thomas	Oliver model	0.96; 0.9; 0.039	0.010
NO01	0.4	0.654	33		10.0	311.0	Gaines-Thomas	Oliver model	0.96; 0.9; 0.039	0.065
PL01	1	1.300	30		25.0	250.0	Gaines-Thomas	Oliver model	0.96; 0.9; 0.039	0.005
PLSNP	0.7	1.300	33		5.0	30.0	Gaines-Thomas	Oliver model	0.96; 0.9; 0.039	0.004
PLTNP	0.5	1.300	33		5.0	60.0	Gaines-Thomas	Oliver model	0.96; 0.9; 0.039	0.004
RS1	0.8	0.768	20		16.7	351.8	Gaines-Thomas	Oliver model	0.96; 0.9; 0.039	0.050
RS2	0.8	1.190	20		13.3	533.9	Gaines-Thomas	Oliver model	0.96; 0.9; 0.039	0.050
SE14	0.8	0.819	4		27.8	21.3	Gaines-Thomas	Mono-protic organic acid	4.5	0.200
SE15	0.7	0.949	4		25.0	9.5	Gaines-Thomas	Mono-protic organic acid	8	0.050
SE16	0.8	0.819	4		21.9	7.1	Gaines-Thomas	Mono-protic organic acid	4.3	0.500

(1) For calceareous soils, fraction (0 - 1) of Ca in parent material: if 0 pure calcite; if 1 pure dolomite.
(2) Type of model used for cation exchange in non-calcareous soils.
(3) Type of model used for simulating dissociation of organic acids (Bonten et al.2016).
(4) Parameters for organic acid dissociation model.

Supplementary Table A5. MetHyd input and output

site	Albedo (1)	Theta_Sat (2)	Theta_FC (3)	Theta_1bar (4)	Theta_WP (5)	Sand_ct (6)	OrgC_ct (7)	Period of data (8)	rf_nit (9)	rf_denit (10)	rf_miR (11)	Theta (12)	Percolation (13)	TempC (14)	Precip (15)
AT01	0.11	0.58	0.43	0.36	0.24	8.80	2.71	1997-2013	0.80	0.80	0.83	0.49	1.23	6.16	1.77
AT09	0.14	0.55			0.24	6.60	1.50	1985-2013	0.92	0.92	1.08	0.40	0.32	8.88	0.72
AT16	0.11	0.65			0.24	43.00	7.30	1985-2013	0.58	0.58	0.63	0.43	0.86	4.22	1.16
BE01								1930-2008	1.10	0.003	1.10				
DE01	0.14	0.56	0.31	0.21	0.08	62.00	0.20	1991-2012	0.74	0.01	0.40	0.32	0.46	5.80	0.97
DE02	0.14	0.42	0.10	0.06	0.02	90.44	0.80	1991-2012	1.06	0.00	0.50	0.11	0.10	7.90	0.60
DE301	0.14	0.45	0.15	0.10	0.04	84.88	1.33	1991-2012	1.01	0.00	0.20	0.13	0.17	8.58	0.70
DE507	0.14	0.50	0.35	0.30	0.20	11.75	2.12	1991-2012	1.02	0.04	0.20	0.35	0.37	8.93	0.98
FI01	0.11	0.55	0.33	0.25	0.14	65.80	0.31	1963-2015							
FI03	0.11	0.45	0.20	0.14	0.06	89.97	0.14	1971-2015							
GB54	0.14	0.52	0.46	0.40	0.28	10.00	3.31	1993-2012	0.49	0.15	0.73	0.38	0.12	9.94	0.73
GB55	0.14	0.52	0.46	0.40	0.28	15.00	2.64	1995-2012	0.50	0.17	0.79	0.39	0.22	10.73	0.83
IT05	0.14	0.59	0.41	0.35	0.23	31.00	3.54	1998-2011							
IT07	0.14	0.53	0.37	0.31	0.21	37.00	3.52	1998-2011							
IT08	0.14	0.48	0.33	0.28	0.19	34.00	1.45	1999-2010							
IT09	0.14	0.50	0.35	0.30	0.20	31.00	2.56	1998-2011							
IT10	0.11	0.58	0.35	0.26	0.12	55.00	1.31	1997-2008							
NO01								1993-2014	0.56	0.07	0.65	0.26	1.02	4.91	1.52
PL01	0.14	0.38	0.26	0.24	0.08			1993-2013	0.76	0.01	0.62	0.19	0.12	6.64	0.66
PLSNP	0.11	0.45	0.14	0.09	0.04	85.00	1.00	1960-2010	0.86	0.00	0.90	0.12	0.23	7.51	0.65
PLTNP	0.11	0.45	0.14	0.09	0.04	85.00	1.00	1960-2010	0.40	0.00	0.42	0.14	1.03	1.46	1.33
RS1	0.11	0.63	0.40	0.31	0.16	59.16	3.90	1990-2014	0.52	0.0001	0.55	0.34	0.47	3.98	0.99
RS2	0.11	0.49	0.29	0.23	0.13	43.58	2.17	1990-2014	0.59	0.00	0.65	0.22	0.20	7.01	0.79
SE14	0.11	0.60	0.43	0.38	0.28	38.84	7.00	1901-2013							
SE15	0.11	0.57	0.40	0.35	0.25	38.01	5.00	1901-2013							
SE16	0.11	0.60	0.42	0.36	0.26	44.43	7.00	1901-2013							

MetHyd inputs

1) Albedo (0 - 1) defaults: conifer 0.11, deciduous 0.14, grassland 0.22
2) Water content at saturation as a volume fraction (0-1), given or computed in MetHyd from soil properties
3) Water content at field capacity (pF 2.0) as a volume fraction (0-1), given or computed in MetHyd from soil properties
4) Water content at -1 bar (pF 3.0) as a volume fraction (0-1), given or computed in MetHyd from soil properties
5) Water content at wilting point (pF 4.2) as a volume fraction (0-1), given or computed in MetHyd from soil properties

6) Sand content of the soil (%)

7) Organic carbon content of the soil (%)

8) Period of meteorological data (monthly or daily values of air temperature, precipitation and radiation) used as input to MetHyd

In addition, MetHyd inputs include site longitude and latitude (Suppl Table A1), bulk density and clay content (%) of the soil (Suppl. Table A3)

MetHyd outputs read by VSD+, either as period average values, or as annual or monthly values

9) Reduction factor of nitrification rates due to moisture and temperatue (-)

10) Reduction factor of denitrification rates due to moisture and temperatue (-)

11) Reduction factor of mineralisation rates due to moisture and temperature (-)

12) Water content of the soil (m3 m3)

13) Precipitation surplus (m/yr)

14) Average temperature T (oC)

15) Precipitation P (m/yr)

Supplementary Table A6. Observed values (N=25) of soil base saturation (BS) at 24 sites, with corresponding modelled values.

Site Code	Observation year	Observed BS	Error of observation used in VSD+ Bayesian calibration	Modelled BS
AT01	2004	1.00	0.10	1.00
AT09	2008	0.25	0.07	0.29
AT16	2008	0.0034	0.001	0.01
BE001	2004	0.08	0.01	0.10
DE01	2010	0.48	0.05	0.42
DE02	2005	0.29	0.18	0.45
DE02	2010	0.48	0.05	0.46
DE301	2007	0.10	0.03	0.23
DE507	2007	0.09	0.01	0.08
FI01	1988	0.37	0.03	0.34
FI03	1988	0.40	0.04	0.35
IT05	2006	0.85	0.11	0.78
IT07	2006	0.43	0.08	0.37
IT08	2006	0.83	0.20	0.67
IT09	2006	0.36	0.13	0.19
IT10	2006	0.25	0.13	0.23
NO01	1991	0.40	0.04	0.22
PL01	1985	0.51	0.05	0.63
PLTPN	2004	0.25	0.11	0.02
PLSPN	2004	0.30	0.01	0.02
RS1	2010	0.07	0.01	0.10
RS2	2013	0.42	0.03	0.47
SE14	2007	0.12	0.03	0.12
SE15	2007	0.06	0.01	0.06
SE16	2007	0.08	0.02	0.01

Supplementary Table A7. Observed values (N=34) of soil carbon to nitrogen ration (C:N) at 23 sites, with corresponding modelled values.

Site Code	Observation year	Observed C:N	Observation error	Modelled C:N
AT01	2004	14.2	1.4	13.66
AT09	2008	9.3	0.9	9.72
AT16	2008	27.6	1.6	27.02
BE001	2004	23.0	1.6	19.20
DE01	1990	21.8	1.0	22.62
DE01	2011	21.7	1.5	20.86
DE02	2005	17.7	1.5	18.54
DE02	2010	15.4	1.5	18.30
DE02	2013	22.1	1.5	18.14
DE301	2007	26.0	0.1	26.03
DE507	2007	19.7	0.1	20.49
FI01	2006	21.6	1.0	22.08
FI03	2006	18.1	1.0	19.50
GB54	1993	9.7	1.0	10.87
GB54	1998	15.4	1.5	10.86
GB54	2003	10.3	1.0	10.85
GB54	2008	10.3	1.0	10.85
GB54	2013	11.7	1.2	10.86
GB55	1994	17.1	1.7	14.67
GB55	1999	16.0	1.6	14.54
GB55	2004	13.0	1.3	14.25
GB55	2009	13.5	1.4	14.08
GB55	2014	13.2	1.3	14.02
IT05	2006	12.9	0.8	15.86
IT07	2006	17.7	4.5	12.16
IT08	2006	17.0	4.0	12.74
IT09	2006	11.5	0.3	10.78
IT10	2006	14.5	3.4	16.02
NO01	1991	31.0	3.5	30.99
PL01	2004	12.0	0.5	10.83
PLTPN	2004	25.0	8.0	29.84
PLSPN	2004	22.0	9.0	19.22
RS1	2010	15.7	1.1	17.88
RS2	2013	11.1	0.5	11.57

Supplementary Table A8. Observed values (N=224) of soil solution pH at 26 sites, with corresponding modelled values.

Site Code	Observation year	Observed annual average pH	Observation error used in VSD+ Bayesian calibration routine	Modelled annual pH
AT01	1998	7.75	1.08	7.17
AT01	1999	7.53	0.44	7.17
AT01	2000	7.50	0.30	7.17
AT01	2001	7.79	0.25	7.17
AT01	2002	7.77	0.26	7.17
AT01	2003	6.78	2.47	7.17
AT01	2004	7.87	0.43	7.17
AT01	2005	7.79	0.20	7.17
AT01	2006	7.85	0.21	7.17
AT01	2007	8.06	0.24	7.17
AT01	2008	8.00	0.18	7.17
AT01	2009	7.84	0.19	7.17
AT01	2010	7.91	0.22	7.17
AT01	2011	7.86	0.17	7.17
AT01	2012	7.93	0.21	7.17
AT09	1998	6.92	0.35	7.02
AT09	1999	7.18	0.31	7.02
AT09	2000	7.26	0.25	7.02
AT09	2001	7.05	0.33	7.03
AT09	2002	7.62	0.37	7.02
AT09	2003	7.64	0.19	7.02
AT09	2004	7.41	0.37	7.02
AT09	2005	6.96	0.19	7.02
AT09	2006	7.06	0.08	7.03
AT09	2007	6.94	0.04	7.03
AT09	2008	7.30	0.10	7.03
AT09	2009	6.80	0.50	7.03
AT09	2010	6.99	0.69	7.03
AT09	2011	6.79	0.33	7.03
AT09	2012	6.88	0.30	7.03
AT16	1998	4.41	0.15	5.09
AT16	1999	4.37	0.11	5.04
AT16	2000	4.58	0.14	4.97
AT16	2001	4.63	0.23	4.93
AT16	2002	4.57	0.25	4.88
AT16	2003	4.46	0.26	4.81
AT16	2004	4.65	0.11	4.75
AT16	2005	4.97	0.02	4.70
AT16	2006	4.99	0.10	5.17
AT16	2007	5.02	0.05	5.13
AT16	2008	4.94	0.02	5.08
AT16	2009	5.23	0.26	5.01
AT16	2010	5.18	0.42	4.94
AT16	2011	5.39	0.26	4.90
BE001	1992	3.62	0.15	3.62
BE001	1993	3.54	0.18	3.65

BE001	1994	3.56	0.18	3.71
BE001	1995	3.48	0.16	3.76
BE001	1996	3.55	0.14	3.64
BE001	1997	3.63	0.16	3.59
BE001	1998	3.72	0.49	3.78
BE001	1999	3.93	0.57	3.75
BE001	2000	3.78	0.09	3.77
BE001	2001	3.83	0.09	3.86
BE001	2002	3.91	0.11	3.88
BE001	2003	3.83	0.09	3.75
BE001	2004	3.86	0.09	3.71
BE001	2005	3.92	0.10	3.70
BE001	2006	3.84	0.07	3.68
BE001	2007	3.67	0.11	3.73
BE001	2008	3.76	0.05	3.79
BE001	2009	3.81	0.12	3.83
BE001	2010	3.92	0.07	3.93
BE001	2011	3.95	0.06	3.91
BE001	2012	3.95	0.06	3.94
BE001	2013	4.02	0.19	3.89
BE001	2014	4.08	0.27	3.91
BE001	2015	4.07	0.12	3.95
DE01	1991	4.68	0.10	4.28
DE01	1992	4.74	0.10	4.30
DE01	1993	4.61	0.10	4.31
DE01	1994	4.50	0.10	4.35
DE01	1995	4.42	0.10	4.37
DE01	1996	4.45	0.10	4.37
DE01	1997	4.37	0.10	4.40
DE01	1998	4.70	0.10	4.42
DE01	1999	4.57	0.10	4.43
DE01	2000	4.57	0.10	4.44
DE01	2001	4.70	0.10	4.45
DE01	2002	4.63	0.10	4.45
DE01	2003	4.70	0.10	4.45
DE01	2004	4.81	0.10	4.43
DE01	2005	4.76	0.10	4.47
DE01	2006	4.80	0.10	4.50
DE01	2007	4.73	0.10	4.49
DE01	2008	4.83	0.10	4.51
DE01	2009	4.84	0.10	4.53
DE01	2010	4.81	0.10	4.49
DE01	2011	4.89	0.10	4.53
DE01	2012	4.86	0.10	4.53
DE02	2005	4.93	1.30	6.14
DE301	1996	4.15	0.26	4.08
DE301	1997	4.13	0.22	4.10
DE301	1998	4.14	0.22	4.12
DE301	1999	4.19	0.21	4.14
DE301	2000	4.24	0.18	4.17
DE301	2001	4.22	0.21	4.18
DE507	1996	4.15	0.26	4.12
DE507	1997	4.13	0.22	4.12
DE507	1998	4.14	0.22	4.13
DE507	1999	4.19	0.21	4.14

DE507	2000	4.24	0.18	4.15
DE507	2001	4.22	0.21	4.16
FI01	2002	4.69	1.50	4.60
FI01	2003	4.19	1.50	4.70
FI01	2004	4.62	1.50	4.78
FI01	2005	4.27	1.50	4.73
FI01	2006	4.43	1.50	4.76
FI03	2002	4.57	1.50	4.21
FI03	2003	4.41	1.50	4.38
FI03	2004	4.46	1.50	4.53
FI03	2005	4.25	1.50	4.31
FI03	2006	4.16	1.50	4.38
GB54	1993	5.84	0.58	5.35
GB54	1998	5.57	0.56	5.45
GB54	2003	5.24	0.52	5.54
GB54	2008	5.69	0.57	5.62
GB54	2013	5.44	0.54	5.69
GB55	1994	4.63	0.46	4.21
GB55	1999	4.66	0.47	4.32
GB55	2004	4.34	0.43	4.44
GB55	2009	4.25	0.42	4.55
GB55	2014	4.56	0.46	4.67
IT05	1999	6.38	0.47	6.16
IT07	2006	8.30	0.87	6.25
IT08	2006	6.21	0.33	4.42
IT09	2006	6.05	0.53	5.43
IT09	2008	5.15	0.76	5.45
IT10	2006	5.75	0.32	5.35
NO01	1993	4.20	0.20	4.12
NO01	1994	4.40	0.20	4.15
NO01	1995	4.30	0.20	4.18
NO01	1996	4.30	0.20	4.18
NO01	1997	4.30	0.20	4.19
NO01	1998	4.40	0.20	4.19
NO01	1999	4.30	0.20	4.20
NO01	2000	4.30	0.20	4.20
NO01	2001	4.30	0.20	4.21
NO01	2002	4.40	0.20	4.22
NO01	2003	4.40	0.20	4.22
NO01	2004	4.40	0.20	4.23
NO01	2005	4.40	0.20	4.23
NO01	2006	4.40	0.20	4.24
NO01	2007	4.40	0.20	4.24
NO01	2008	4.40	0.20	4.25
NO01	2009	4.40	0.20	4.26
NO01	2010	4.40	0.20	4.26
NO01	2011	4.40	0.20	4.27
NO01	2012	4.50	0.20	4.27
NO01	2013	4.50	0.20	4.27
NO01	2014	4.40	0.20	4.28
PL01	1995	5.10	0.30	5.48
PL01	1996	4.70	0.30	5.50
PL01	1997	5.30	0.30	5.52
PL01	2012	5.60	0.30	5.70
PL01	2013	5.70	0.30	5.70

PLTPN	1998	4.20	0.30	4.30
PLTPN	2004	4.50	0.30	4.30
PLTPN	2012	4.50	0.30	4.30
PLSPN	1998	4.60	0.20	4.30
PLSPN	2004	4.80	0.20	4.09
PLSPN	2012	4.80	0.20	4.16
RS1	2011	6.35	0.70	4.54
RS1	2012	5.87	0.75	4.55
RS1	2013	4.62	0.76	4.56
RS1	2014	5.60	0.52	4.58
RS1	2015	5.82	1.21	4.60
RS1	2016	5.48	0.62	4.61
RS2	2014	6.09	1.03	5.66
RS2	2015	6.42	0.86	5.66
RS2	2016	6.02	0.46	5.66
SE14	1994	4.69	0.51	4.31
SE14	1995	4.61	0.32	4.33
SE14	1996	4.56	0.22	4.31
SE14	1997	4.47	0.17	4.33
SE14	1998	4.59	0.16	4.37
SE14	1999	4.68	0.30	4.37
SE14	2000	4.67	0.30	4.38
SE14	2001	4.70	0.34	4.40
SE14	2002	4.71	0.30	4.40
SE14	2003	4.79	0.20	4.39
SE14	2004	4.75	0.24	4.42
SE14	2005	4.72	0.18	4.42
SE14	2006	4.74	0.24	4.43
SE14	2007	4.75	0.19	4.45
SE14	2008	4.85	0.26	4.46
SE14	2009	4.95	0.37	4.46
SE14	2010	4.85	0.23	4.47
SE14	2011	4.62	0.27	4.49
SE14	2012	4.81	0.30	4.50
SE14	2013	4.26	0.58	4.49
SE15	1994	4.60	0.14	4.16
SE15	1995	4.63	0.11	4.19
SE15	1996	4.66	0.07	4.17
SE15	1997	4.68	0.08	4.19
SE15	1998	4.62	0.14	4.23
SE15	1999	4.71	0.10	4.28
SE15	2000	4.73	0.09	4.35
SE15	2001	4.71	0.08	4.37
SE15	2002	4.74	0.11	4.36
SE15	2003	4.52	0.54	4.35
SE15	2004	4.60	0.31	4.41
SE15	2005	4.64	0.31	4.40
SE15	2006	4.69	0.22	4.44
SE15	2007	4.76	0.15	4.44
SE15	2008	4.80	0.15	4.50
SE15	2009	4.86	0.09	4.50
SE15	2010	4.92	0.08	4.50
SE15	2011	4.88	0.07	4.49
SE15	2012	4.91	0.11	4.54
SE15	2013	4.80	0.09	4.45

SE16	2000	5.19	0.26	5.12
SE16	2001	5.24	0.30	5.12
SE16	2002	5.18	0.27	5.12
SE16	2003	5.13	0.51	5.12
SE16	2004	4.97	0.55	5.12
SE16	2005	5.18	0.42	5.12
SE16	2007	5.14	0.44	5.13
SE16	2008	4.87	0.72	5.13
SE16	2009	5.16	0.72	5.13
SE16	2010	5.44	0.21	5.13
SE16	2011	5.11	0.44	5.13
SE16	2012	5.15	0.52	5.13
SE16	2013	4.94	0.76	5.13

Supplementary Table A9. Calibrated VSD+ parameter values.

Site	Initial C pool (g m^{-2})	Initial C:N (g g^{-1})	lgK_AlBc (1)	lgK_HBc (2)	lgK_Alox (3)	Initial BS (4)	Ca weathering (eq m^3 yr^{-1})	Mg weathering (eq m^3 yr^{-1})	K weathering (eq m^3 yr^{-1})	Na weathering (eq m^3 yr^{-1})
AT01	6015	5	-	-	6.15	-	10.000	10.000		
AT09	9000	8	16.43	2.57	8.90	-	0.468	0.304	0.309	
AT16	28000	23	6.82	3.47	8.00	-	0.010	0.010	0.100	
BE001	14657	35	-0.89	-1.09	7.46	-	0.010	0.001	0.001	0.003
DE01	7000	28	0.17	2.03	7.90	0.60	0.150	0.200	0.150	
DE02	27516	21	0.14	2.00	7.89	0.67	0.200	0.010	0.093	0.0004
DE301	10000	34	0.10	2.67	7.90	0.26	0.006	0.006	0.011	
DE507	10370	22	0.75	2.08	7.90	0.20	0.108	0.053	0.116	
FI01	1200	5	0.50	6.30	6.00	0.35	0.060	0.070	0.020	0.020
FI03	300	2	-5.00	1.00	7.00	0.45	0.025	0.008	0.008	0.008
GB54	11850	10	0.16	6.73	7.90	-	0.173	0.035	0.025	0.025
GB55	15032	18	0.16	6.73	7.90	-	0.294	0.148	0.025	0.025
IT05	4480	10	8.50	2.00	8.00	0.70	0.014	0.007	0.004	0.002
IT07	2000	15	12.00	3.00	8.00	0.60	0.055	0.022	0.014	0.024
IT08	8000	15	-5.00	0.21	8.00	0.60	0.011	0.004	0.005	0.049
IT09	14000	8	6.97	3.77	8.00	0.33	0.032	0.013	0.008	0.014
IT10	3033	20	4.26	2.53	8.00	0.34	0.023	0.009	0.006	0.010
NO01	10453	52	0.10	1.98	6.22	0.29	0.050	0.004	0.004	0.012
PL01	7000	8	3.00	7.00	6.00	0.40	0.800	0.100		
PLSNP	5093	25	0.001	0.07	7.90	0.10	0.005		0.001	0.001
PLTNP	6650	20	0.003	0.003	7.90	0.20	0.020		0.001	0.001
RS1	6358	10	5.02	2.21	6.00	0.07	0.083			
RS2	5793	10	0.30	2.08	8.00	0.46	0.100			
SE14	8000	25	0.16	3.80	7.90	0.20	0.020	0.030	0.010	0.010
SE15	10000	25	0.16	3.80	7.90	-	0.020	0.012	0.002	0.010
SE16	5000	25	0.16	4.00	7.90	0.10	0.020	0.010	0.001	0.010

(1) Log10 of selectivity constant for Al-Bc exchange
(2) Log10 of selectivity constant for H-Bc exchange
(3) Log10 of Al equilibrium constant ((mol/l) $^{-2}$)
(4) Initial base saturation. If missing, its value is determined by the model assuming equilibrium conditions at the start.

Supplementary Table A10. Observed values (N=171) of soil solution [NO$_3^-$] at 11 sites, with corresponding modelled values.

Site	Observation year	Observed annual average [NO$_3^-$] (µeq L^{-1})	Modelled annual [NO$_3^-$] (µeq L^{-1})
AT01	1998	66.68	7.80
AT01	1999	100.45	7.63
AT01	2000	66.87	7.48
AT01	2001	69.20	7.40
AT01	2002	37.35	7.34
AT01	2003	69.14	7.28
AT01	2004	48.56	7.21
AT01	2005	47.75	7.14
AT01	2006	45.66	7.24
AT01	2007	41.11	7.34
AT01	2008	65.24	7.43
AT01	2009	56.74	7.53
AT01	2010	39.99	7.64
AT01	2011	51.82	7.63
AT01	2012	61.44	7.63
AT09	1998	60.00	7.06
AT09	1999	70.00	6.90
AT09	2000	60.00	6.72
AT09	2001	30.00	6.65
AT09	2002	40.00	6.60
AT09	2003	80.00	6.52
AT09	2004	90.00	6.46
AT09	2005	40.00	6.39
AT09	2006	40.00	6.32
AT09	2007	20.00	6.22
AT09	2008	20.00	6.15
AT09	2009	50.00	6.07
AT09	2010	30.00	6.00
AT09	2011	50.00	5.88
AT09	2012	30.00	5.76
AT16	1998	140.00	1.37
AT16	1999	160.00	1.37
AT16	2000	140.00	1.35
AT16	2001	60.00	1.28
AT16	2002	40.00	1.22
AT16	2003	40.00	1.16
AT16	2004	20.00	1.08
AT16	2005	30.00	1.02
AT16	2006	20.00	0.95
AT16	2007	20.00	0.85
AT16	2008	20.00	0.78
AT16	2009	0.01	0.71
AT16	2010	40.00	0.65
AT16	2011	0.01	0.63
BE001	1992	1060.00	582.54
BE001	1993	1140.00	464.84
BE001	1994	840.00	284.64
BE001	1995	730.00	48.42

BE001	1996	1260.00	105.27
BE001	1997	970.00	128.34
BE001	1998	650.00	34.13
BE001	1999	260.00	57.72
BE001	2000	430.00	238.81
BE001	2001	380.00	39.76
BE001	2002	360.00	92.86
BE001	2003	410.00	178.49
BE001	2004	190.00	287.97
BE001	2005	250.00	333.01
BE001	2006	290.00	320.98
BE001	2007	440.00	158.82
BE001	2008	370.00	141.90
BE001	2009	240.00	79.54
BE001	2010	160.00	32.19
BE001	2011	120.00	40.67
BE001	2012	180.00	31.85
BE001	2013	110.00	39.29
BE001	2014	60.00	32.46
BE001	2015	90.00	30.85
FI01	2002	1.00	8.50
FI01	2004	0.00	2.94
FI01	2006	2.00	4.59
FI03	2002	0.40	6.92
FI03	2003	1.40	3.49
FI03	2004	0.40	2.06
FI03	2005	0.90	5.34
FI03	2006	1.70	3.88
NO01	1993	2.86	8.30
NO01	1994	1.52	7.90
NO01	1995	1.95	7.50
NO01	1996	1.02	7.40
NO01	1997	0.87	7.30
NO01	1998	1.59	7.20
NO01	1999	2.14	7.11
NO01	2000	1.43	7.01
NO01	2001	1.43	6.92
NO01	2002	2.14	6.82
NO01	2003	2.14	6.73
NO01	2004	2.14	6.63
NO01	2005	2.14	6.54
NO01	2006	2.14	6.39
NO01	2007	2.14	6.24
NO01	2008	2.14	6.09
NO01	2009	2.14	5.94
NO01	2010	2.14	5.79
NO01	2011	2.50	5.68
NO01	2012	2.14	5.58
NO01	2013	2.14	5.48
NO01	2014	2.14	5.37
PL01	1995	163.00	28.63
PL01	1996	141.00	27.70
PL01	1997	19.00	26.81
PL01	2012	5.00	23.38
PL01	2013	11.00	23.14

RS1	2011	316.00	12.426
RS1	2012	1058.00	12.158
RS1	2013	149.00	11.901
RS1	2014	128.00	11.612
RS1	2015	58.00	11.354
RS1	2016	111.00	11.083
RS2	2014	225.00	12.928
RS2	2015	95.00	12.936
RS2	2016	77.00	12.95
SE14	1994	0.33	7.71
SE14	1995	1.09	7.38
SE14	1996	3.12	9.02
SE14	1997	0.87	7.91
SE14	1998	0.15	5.94
SE14	1999	0.16	6.52
SE14	2000	0.17	6.78
SE14	2001	0.23	6.44
SE14	2002	0.25	7.02
SE14	2003	0.37	7.10
SE14	2004	0.15	5.22
SE14	2005	0.38	6.28
SE14	2006	0.68	5.30
SE14	2007	0.16	4.39
SE14	2008	0.21	3.72
SE14	2009	0.22	4.30
SE14	2010	4.24	3.61
SE14	2011	8.18	3.77
SE14	2012	20.97	3.28
SE14	2013	42.16	4.26
SE14	2014	7.93	4.14
SE14	2015	10.03	4.00
SE15	1994	0.55	3.16
SE15	1995	0.40	2.79
SE15	1996	1.32	3.25
SE15	1997	0.28	3.02
SE15	1998	0.60	2.49
SE15	1999	0.10	2.22
SE15	2000	0.19	1.83
SE15	2001	0.38	2.45
SE15	2002	0.41	2.33
SE15	2003	0.25	2.40
SE15	2004	0.27	1.74
SE15	2005	0.31	1.92
SE15	2006	0.50	1.56
SE15	2007	0.14	1.44
SE15	2008	0.19	1.06
SE15	2009	0.09	1.14
SE15	2010	0.15	1.11
SE15	2011	0.09	1.20
SE15	2012	0.09	0.98
SE15	2013	0.12	1.53
SE15	2014	0.11	1.49
SE15	2015	0.23	1.43
SE16	2000	0.14	1.41
SE16	2001	0.31	1.59

SE16	2002	0.22	1.89
SE16	2003	0.24	2.08
SE16	2004	0.27	1.77
SE16	2005	0.34	1.56
SE16	2007	0.07	0.99
SE16	2008	0.09	0.82
SE16	2009	0.10	0.99
SE16	2010	0.09	1.03
SE16	2011	0.06	0.87
SE16	2012	0.11	0.77
SE16	2013	0.15	0.90
SE16	2014	0.12	0.87
SE16	2015	0.11	0.83

Supplementary Table A11. Observed values (N=97) of soil solution [NH$_4^+$] at 6 sites, with corresponding modelled values.

Site	Observation year	Observed annual average [NH$_4$] (µeq L^{-1})	Modelled annual [NH$_4$] (µeq L^{-1})
FI01	2002	2.00	0.23
FI01	2004	3.00	0.07
FI01	2006	1.00	0.42
FI03	2002	10.00	0.20
FI03	2003	20.00	0.18
FI03	2004	10.00	0.06
FI03	2005	20.00	0.37
FI03	2006	4.00	0.23
NO01	1993	3.01	0.41
NO01	1994	2.41	0.39
NO01	1995	2.66	0.37
NO01	1996	1.53	0.37
NO01	1997	4.12	0.37
NO01	1998	2.62	0.37
NO01	1999	2.94	0.37
NO01	2000	3.81	0.37
NO01	2001	4.08	0.37
NO01	2002	5.51	0.37
NO01	2003	5.10	0.37
NO01	2004	4.59	0.37
NO01	2005	6.63	0.37
NO01	2006	5.00	0.37
NO01	2007	4.46	0.36
NO01	2008	2.02	0.36
NO01	2009	2.50	0.36
NO01	2010	4.08	0.35
NO01	2011	6.16	0.35
NO01	2012	2.32	0.35
NO01	2013	5.35	0.35
NO01	2014	3.30	0.35
RS1	2012	250.00	0.80
RS1	2013	243.00	0.80
RS1	2014	308.00	0.81
RS1	2015	133.00	0.82
RS1	2016	148.00	0.82
RS2	2014	190.00	0.66
RS2	2015	24.00	0.66
RS2	2016	45.00	0.66
SE14	1994	2.70	0.13
SE14	1995	2.34	0.16
SE14	1996	2.67	0.27
SE14	1997	1.36	0.15

SE14	1998	0.51	0.21
SE14	1999	1.64	0.14
SE14	2000	1.56	0.15
SE14	2001	1.45	0.17
SE14	2002	1.50	0.13
SE14	2003	2.62	0.17
SE14	2004	7.50	0.15
SE14	2005	2.26	0.15
SE14	2006	2.29	0.07
SE14	2007	1.61	0.11
SE14	2008	1.48	0.08
SE14	2009	1.97	0.11
SE14	2010	3.99	0.11
SE14	2011	5.19	0.07
SE14	2012	3.43	0.10
SE14	2013	5.55	0.10
SE14	2014	3.13	0.10
SE14	2015	2.64	0.10
SE15	1994	0.58	1.20
SE15	1995	0.56	1.10
SE15	1996	0.90	1.37
SE15	1997	0.25	1.21
SE15	1998	0.41	1.19
SE15	1999	1.22	1.05
SE15	2000	0.39	0.90
SE15	2001	0.36	1.16
SE15	2002	0.27	1.01
SE15	2003	0.89	1.04
SE15	2004	0.97	0.75
SE15	2005	0.97	0.77
SE15	2006	0.79	0.58
SE15	2007	0.50	0.62
SE15	2008	0.78	0.46
SE15	2009	0.55	0.51
SE15	2010	1.39	0.51
SE15	2011	0.73	0.50
SE15	2012	1.19	0.44
SE15	2013	1.15	0.64
SE15	2014	0.70	0.64
SE15	2015	1.75	0.63
SE16	2000	0.35	0.08
SE16	2001	0.39	0.09
SE16	2002	0.30	0.06
SE16	2003	0.49	0.08
SE16	2004	0.50	0.09
SE16	2005	0.33	0.07
SE16	2007	0.30	0.04
SE16	2008	0.14	0.04
SE16	2009	0.28	0.04
SE16	2010	0.18	0.04

SE16	2011	0.07	0.02
SE16	2012	0.56	0.04
SE16	2013	0.22	0.03
SE16	2014	0.38	0.03
SE16	2015	0.30	0.03

SE16	2011	0.07	0.02
SE16	2012	0.56	0.04
SE16	2013	0.22	0.03
SE16	2014	0.38	0.03
SE16	2015	0.30	0.03

Supplementary Table A12. Observed values (N=144) of soil solution $[SO_4^{2-}]$ at 9 sites, with corresponding modelled values.

Site	Observation year	Observed annual average $[SO_4^{2-}]$ (μeq L^{-1})	Modelled annual $[SO_4^{2-}]$ (μeq L^{-1})
AT01	1998	26.9	44.3
AT01	1999	41.8	36.8
AT01	2000	43.5	29.4
AT01	2001	52.2	28.2
AT01	2002	29.8	28.0
AT01	2003	39.8	28.0
AT01	2004	30.0	28.0
AT01	2005	30.2	28.0
AT01	2006	35.3	26.4
AT01	2007	26.0	24.4
AT01	2008	25.9	22.4
AT01	2009	25.4	20.5
AT01	2010	32.5	18.5
AT01	2011	32.0	18.1
AT01	2012	36.5	18.1
AT09	1998	640.0	147.9
AT09	1999	600.0	128.0
AT09	2000	610.0	108.1
AT09	2001	500.0	97.9
AT09	2002	600.0	91.9
AT09	2003	720.0	87.6
AT09	2004	630.0	84.0
AT09	2005	520.0	80.8
AT09	2006	430.0	76.8
AT09	2007	480.0	72.6
AT09	2008	510.0	68.3
AT09	2009	350.0	63.9
AT09	2010	310.0	59.4
AT09	2011	330.0	56.3
AT09	2012	370.0	53.6
AT16	1998	170.0	27.4
AT16	1999	130.0	25.5
AT16	2000	130.0	23.6
AT16	2001	100.0	22.5
AT16	2002	110.0	21.7
AT16	2003	110.0	20.9
AT16	2004	120.0	20.0
AT16	2005	120.0	19.2
AT16	2006	110.0	16.9
AT16	2007	100.0	14.3
AT16	2008	110.0	11.7
AT16	2009	70.0	9.1

AT16	2010	110.0	6.4
AT16	2011	80.0	5.7
BE001	1992	1270.0	1365.9
BE001	1993	910.0	1176.5
BE001	1994	550.0	859.9
BE001	1995	440.0	757.3
BE001	1996	880.0	1495.6
BE001	1997	990.0	2057.1
BE001	1998	1260.0	746.2
BE001	1999	520.0	861.1
BE001	2000	510.0	660.8
BE001	2001	370.0	518.8
BE001	2002	350.0	410.5
BE001	2003	340.0	807.8
BE001	2004	430.0	801.4
BE001	2005	610.0	877.0
BE001	2006	670.0	1001.1
BE001	2007	910.0	798.0
BE001	2008	500.0	589.4
BE001	2009	620.0	511.0
BE001	2010	470.0	301.2
BE001	2011	360.0	327.2
BE001	2012	310.0	291.3
BE001	2013	340.0	323.2
BE001	2014	360.0	292.1
BE001	2015	300.0	233.7
FI01	2002	280.0	107.6
FI01	2004	250.0	38.3
FI01	2006	230.0	57.9
FI03	2002	80.0	88.4
FI03	2003	60.0	48.2
FI03	2004	70.0	25.5
FI03	2005	100.0	61.3
FI03	2006	60.0	48.9
RS1	2011	1174.0	310.57
RS1	2012	1671.0	292.52
RS1	2013	807.0	271.94
RS1	2014	789.0	250.45
RS1	2015	991.0	228.61
RS1	2016	317.0	206.66
RS2	2014	821.0	323.28
RS2	2015	721.0	322.87
RS2	2016	173.0	322.67
SE14	1994	493.9	151.7
SE14	1995	308.7	130.6
SE14	1996	247.2	149.2
SE14	1997	257.8	134.3
SE14	1998	231.6	95.7
SE14	1999	209.7	87.7
SE14	2000	223.4	84.6

SE14	2001	193.4	78.5
SE14	2002	162.0	81.8
SE14	2003	155.8	84.1
SE14	2004	211.2	62.4
SE14	2005	175.6	64.7
SE14	2006	154.0	56.2
SE14	2007	106.9	46.0
SE14	2008	117.6	36.7
SE14	2009	110.7	38.3
SE14	2010	99.1	32.7
SE14	2011	84.1	31.0
SE14	2012	66.0	26.0
SE14	2013	103.4	30.7
SE14	2014	159.0	31.7
SE14	2015	165.3	31.1
SE15	1994	230.0	130.7
SE15	1995	191.8	105.5
SE15	1996	193.9	112.4
SE15	1997	186.1	102.1
SE15	1998	171.2	83.1
SE15	1999	160.7	66.6
SE15	2000	150.7	49.0
SE15	2001	123.1	58.1
SE15	2002	129.2	57.4
SE15	2003	133.5	58.1
SE15	2004	119.1	42.6
SE15	2005	106.8	40.0
SE15	2006	106.3	31.9
SE15	2007	98.1	29.9
SE15	2008	97.1	22.8
SE15	2009	93.6	21.8
SE15	2010	88.9	20.7
SE15	2011	92.8	21.0
SE15	2012	90.1	17.0
SE15	2013	99.4	23.5
SE15	2014	84.6	25.5
SE15	2015	96.7	25.5
SE16	2000	41.1	24.0
SE16	2001	31.9	22.9
SE16	2002	30.7	27.0
SE16	2003	31.6	30.6
SE16	2004	30.0	28.1
SE16	2005	25.6	24.1
SE16	2007	26.8	15.4
SE16	2008	21.9	12.9
SE16	2009	22.0	13.5
SE16	2010	19.2	14.0
SE16	2011	16.7	11.9
SE16	2012	15.9	9.9
SE16	2013	16.9	10.4

| SE16 | 2014 | 23.2 | 10.3 |
| SE16 | 2015 | 25.4 | 10.0 |

Table A13. Observed values (N=100) of soil solution [Bc^{2+}] at 6 sites, with corresponding modelled values. Bc is the sum of Ca, Mg and K, where two K^+ ions are treated as one divalent ion.

Site	Observation year	Observed annual average Bc (μeq L^{-1})	Modelled annual Bc (μeq L^{-1})
BE001	1992	720.0	524.7
BE001	1993	730.0	450.5
BE001	1994	470.0	340.6
BE001	1995	530.0	265.4
BE001	1996	590.0	453.2
BE001	1997	530.0	563.2
BE001	1998	520.0	230.4
BE001	1999	320.0	257.3
BE001	2000	330.0	298.6
BE001	2001	220.0	199.4
BE001	2002	200.0	186.6
BE001	2003	150.0	332.6
BE001	2004	160.0	384.9
BE001	2005	190.0	415.9
BE001	2006	210.0	451.6
BE001	2007	260.0	353.0
BE001	2008	200.0	276.0
BE001	2009	200.0	228.8
BE001	2010	130.0	142.5
BE001	2011	80.0	156.4
BE001	2012	140.0	133.3
BE001	2013	130.0	168.1
BE001	2014	140.0	153.8
BE001	2015	100.0	130.4
FI01	2002	180.0	77.3
FI01	2004	160.0	58.0
FI01	2006	160.0	59.4
FI03	2002	80.0	3.9
FI03	2003	170.0	1.7
FI03	2004	70.0	0.9
FI03	2005	90.0	2.4
FI03	2006	130.0	1.8
RS1	2011	2001.0	337.0
RS1	2012	566.0	320.7
RS1	2013	423.0	301.3
RS1	2014	239.0	280.8
RS1	2015	26.0	260.4
RS1	2016	223.0	239.6
RS2	2014	875.0	449.1
RS2	2015	68.0	448.8
RS2	2016	368.0	448.7
SE14	1994	323.0	174.3
SE14	1995	173.0	159.8

SE14	1996	190.0	175.0
SE14	1997	193.0	164.0
SE14	1998	145.0	134.9
SE14	1999	107.0	129.8
SE14	2000	117.0	127.9
SE14	2001	95.0	130.3
SE14	2002	105.0	133.6
SE14	2003	100.0	136.1
SE14	2004	104.0	118.8
SE14	2005	97.0	122.2
SE14	2006	65.0	115.9
SE14	2007	74.0	108.2
SE14	2008	70.0	101.4
SE14	2009	65.0	103.9
SE14	2010	96.0	99.3
SE14	2011	156.0	103.4
SE14	2012	163.0	99.0
SE14	2013	290.0	104.3
SE14	2014	203.0	105.7
SE14	2015	242.0	105.7
SE15	1994	75.0	37.7
SE15	1995	50.0	32.7
SE15	1996	59.0	36.6
SE15	1997	48.0	34.8
SE15	1998	41.0	29.4
SE15	1999	41.0	24.4
SE15	2000	34.0	18.3
SE15	2001	32.0	42.4
SE15	2002	32.0	43.3
SE15	2003	33.0	45.9
SE15	2004	28.0	34.4
SE15	2005	28.0	34.9
SE15	2006	26.0	29.0
SE15	2007	30.0	29.1
SE15	2008	27.0	23.1
SE15	2009	32.0	23.3
SE15	2010	25.0	22.9
SE15	2011	33.0	24.3
SE15	2012	30.0	19.6
SE15	2013	30.0	30.2
SE15	2014	28.0	34.5
SE15	2015	33.0	36.1
SE16	2000	37.0	41.2
SE16	2001	26.0	40.0
SE16	2002	23.0	44.6
SE16	2003	30.0	50.7
SE16	2004	31.0	53.3
SE16	2005	32.0	54.4
SE16	2007	30.0	51.4
SE16	2008	30.0	50.5

SE16	2009	37.0	53.7
SE16	2010	26.0	56.7
SE16	2011	35.0	54.8
SE16	2012	51.0	50.9
SE16	2013	24.0	52.1
SE16	2014	29.0	52.8
SE16	2015	21.0	53.3

Supplementary Figures STOTEN-270809
Modelling study of soil C, N and pH response to air pollution and climate change using
European LTER site observations

Holmberg, M., Aherne, J., Austnes, K., Beloica, J., De Marco, A., Dirnböck, T., Fornasier, M.F., Goergen, K., Futter, M., Lindroos, A.-J., Krám, P., Neirynck, J., Nieminen, T.M., Pecka, T., Posch, M., Pröll, G., Rowe, E.C., Scheuschner, T., Schlutow, A., Valinia, S., Forsius, M.

Table of contents:

Figure A9b. Time plots of simulated soil solution pH with 24 climate change scenarios, twelve representing climate forcing level RCP4.5 (light blue) and twelve RCP8.5 (orange).

Supplementary Figure A1. Modelled versus observed values of soil solution concentrations of base cations (BC = Ca + Mg + K) (meq L^{-1}), sulphate SO$_4$$^{2-}$ (meq L^{-1}), nitrate NO$_3$$^{-}$ (meq L^{-1}) and ammonium NH$_4$$^{+}$ (µeq L^{-1}). Dashed line represents 1:1. Number of observations (N) and coefficient of determination (R^2) shown.
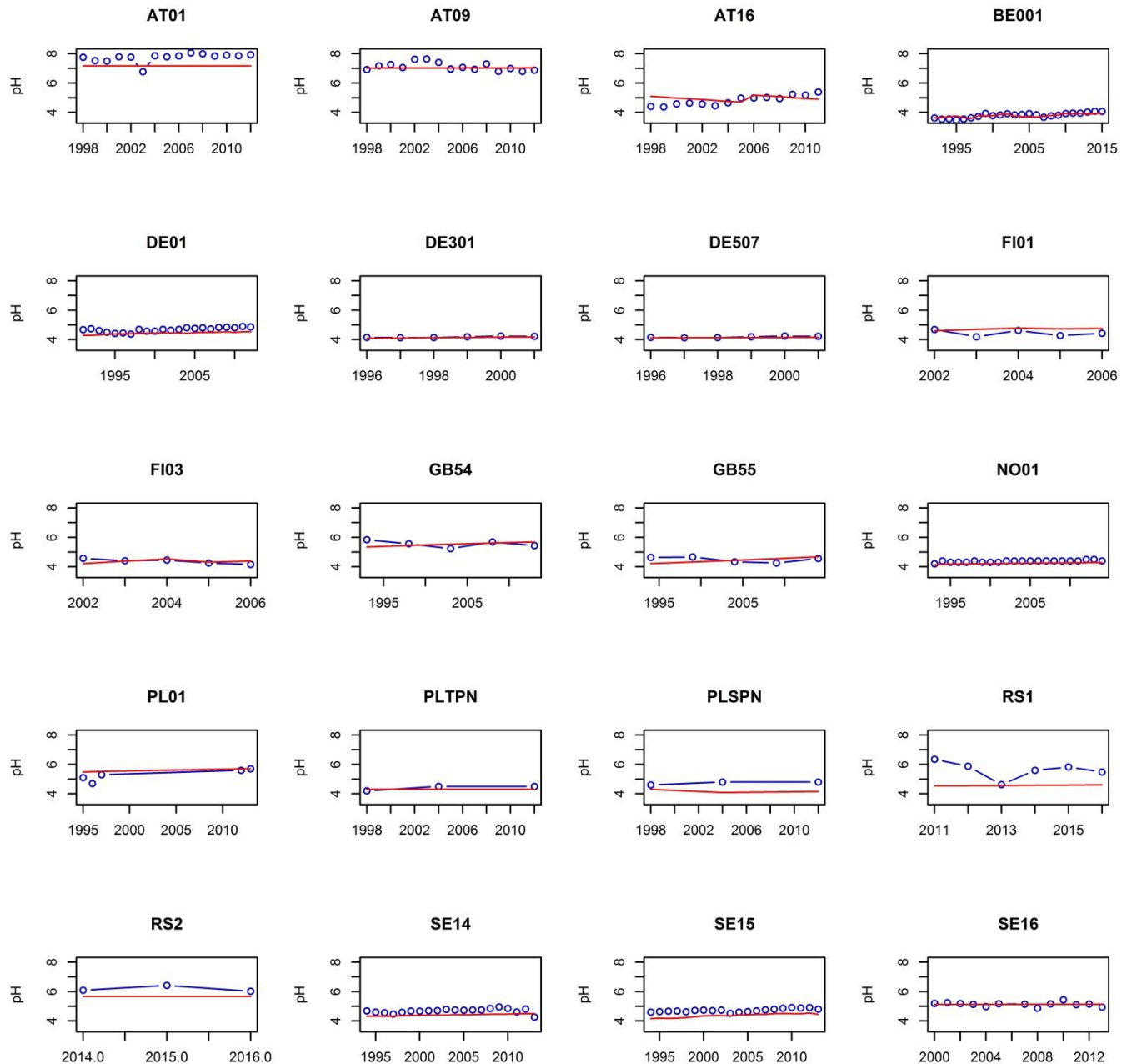
Supplementary Figure A2. Time plots of observed (blue broken line) and modelled (red solid line)

values of soil solution pH at those 20 sites for which there are at least three years of observations.
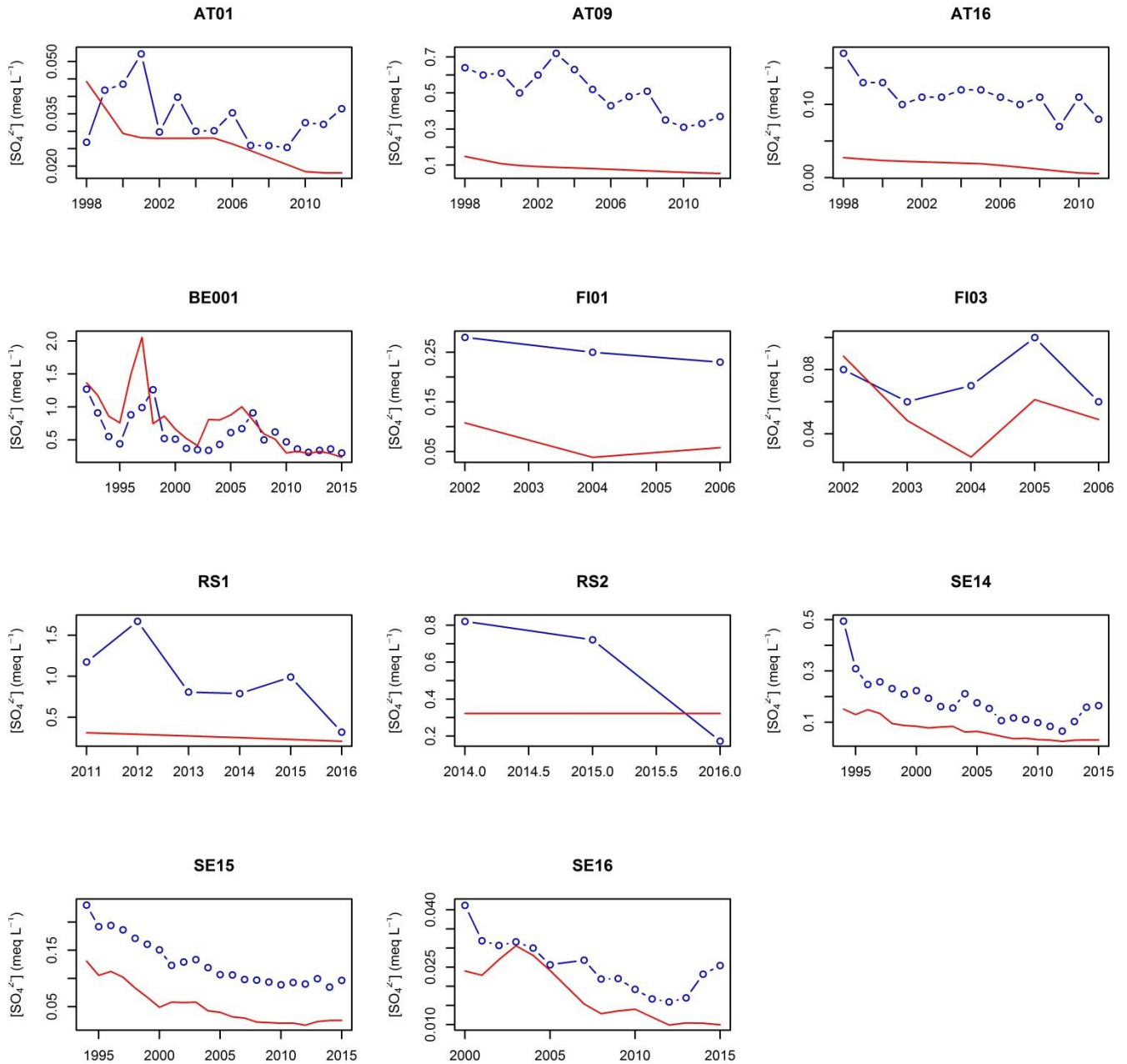
Supplementary Figure A3. Time plots of observed (blue broken line) and modelled (red solid line) values of soil solution sulphate concentrations $[SO_4^{2-}]$ (meq L^{-1}) at those 11 sites for which there are at least three years of observations.
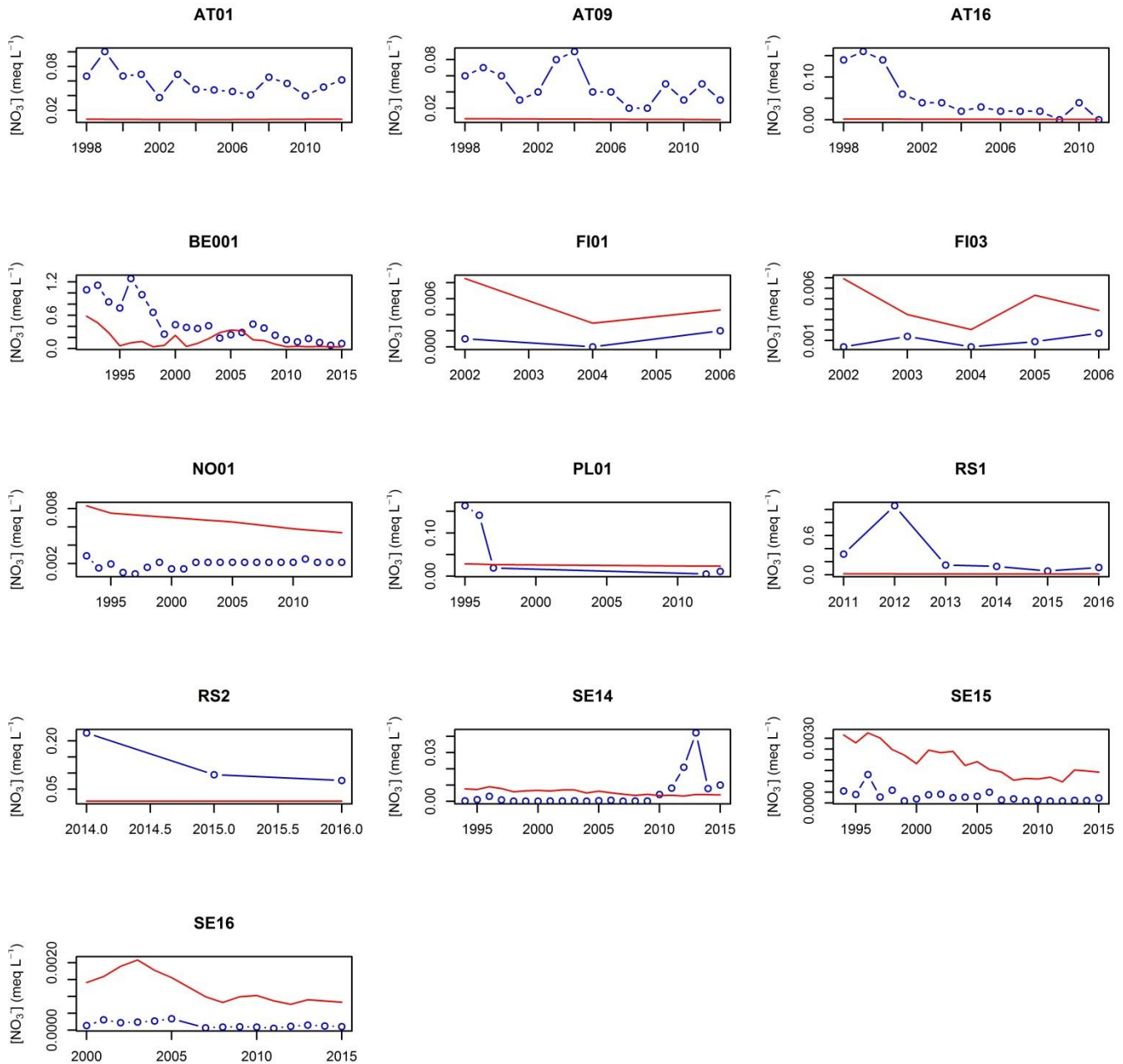
Supplementary Figure A4. Time plots of observed (blue broken line) and modelled (red solid line) values of soil solution nitrate concentrations [NO_3^-] (meq L^{-1}) at those 13 sites for which there are at least three years of observations.
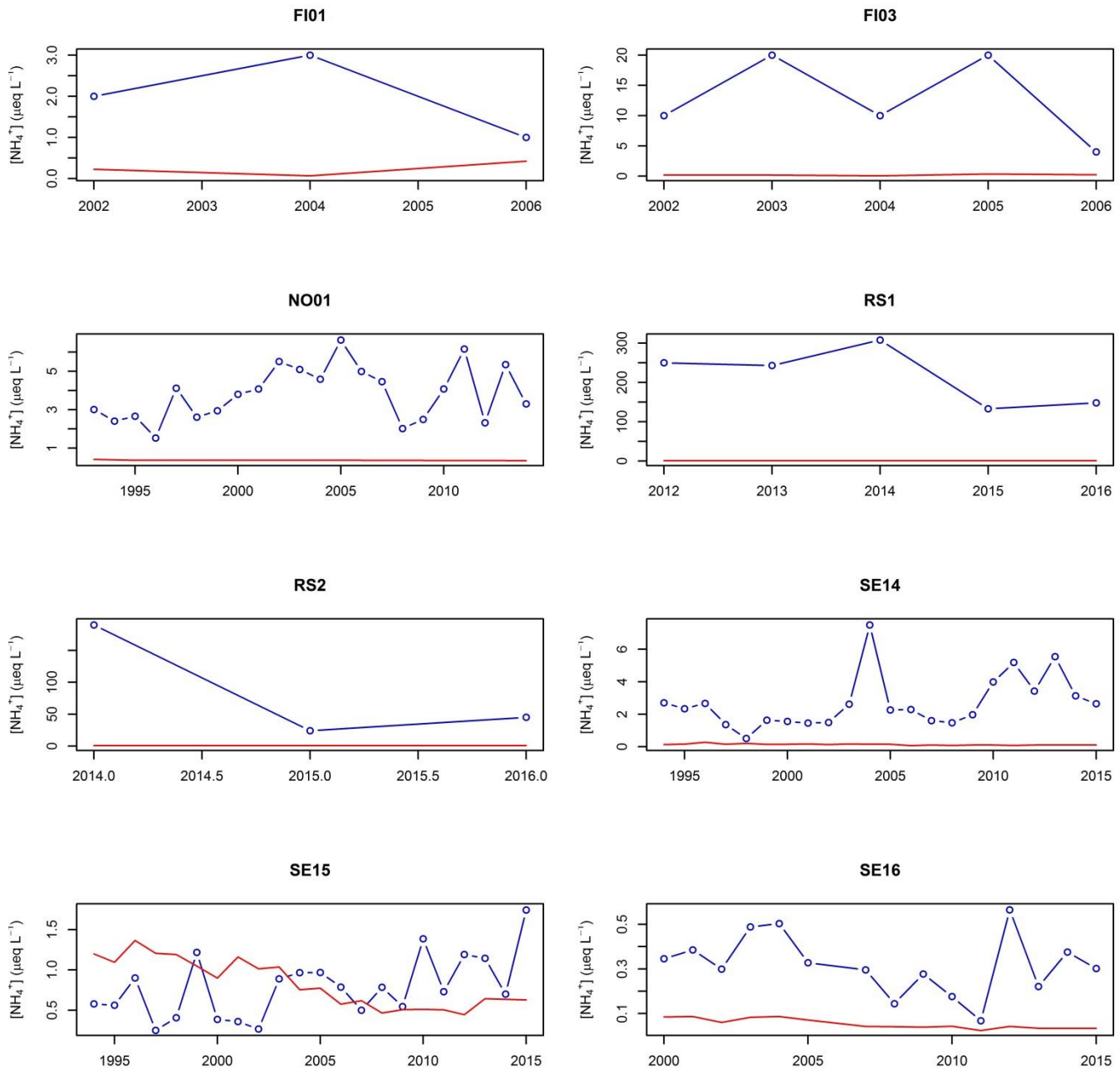
Supplementary Figure A5. Time plots of observed (blue broken line) and modelled (red solid line) values of soil solution nitrate concentrations [NH$_4^+$] (µeq L^{-1}) at those 8 sites for which there are at least three years of observations.
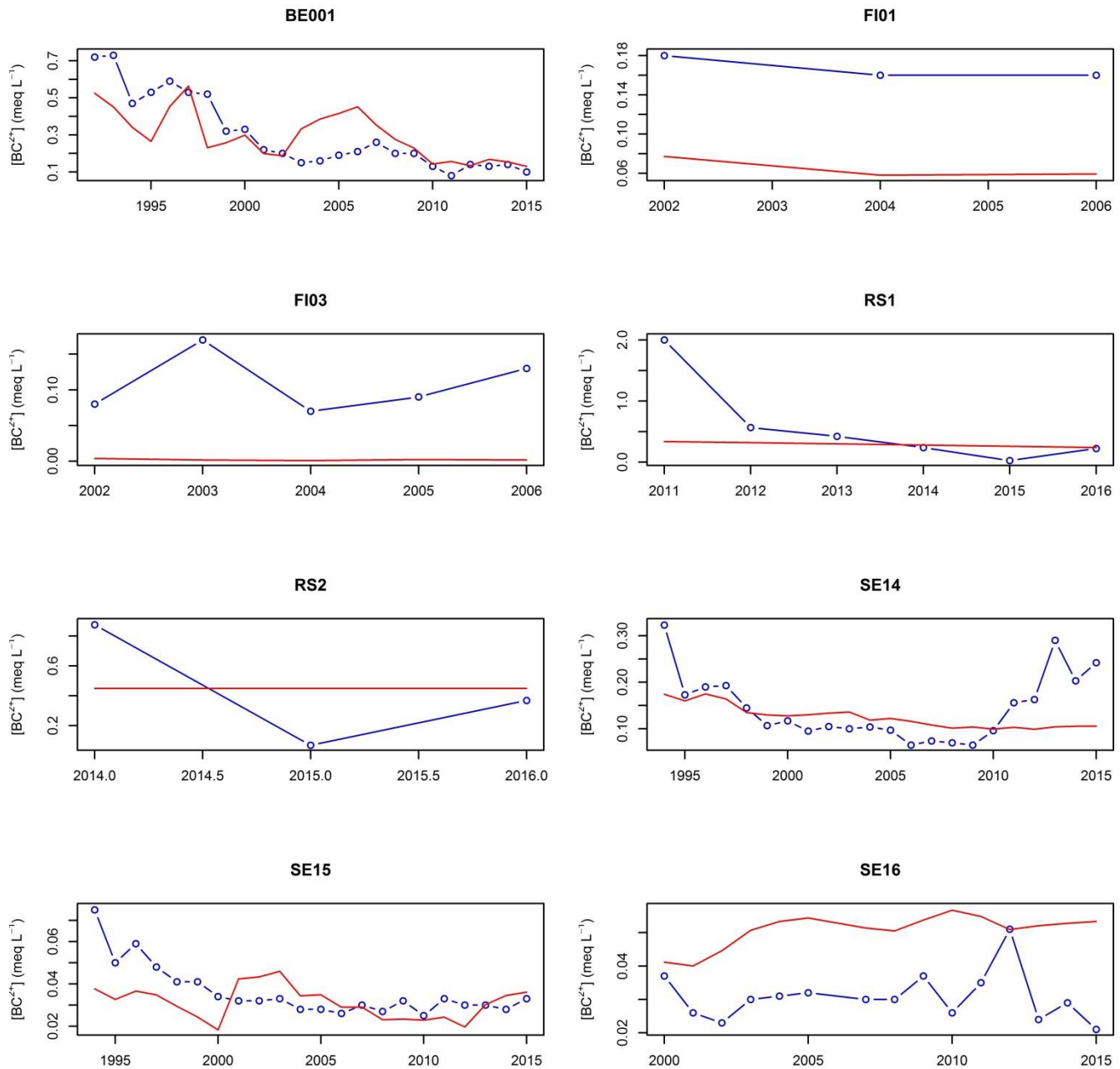
Supplementary Figure A6. Time plots of observed (blue broken line) and modelled (red solid line)

values of soil solution base cation concentrations (sum of calcium, magnesium and potassium)

$[BC^{2+}]$ (meq L^{-1}) at those 8 sites for which there are at least three years of observations.
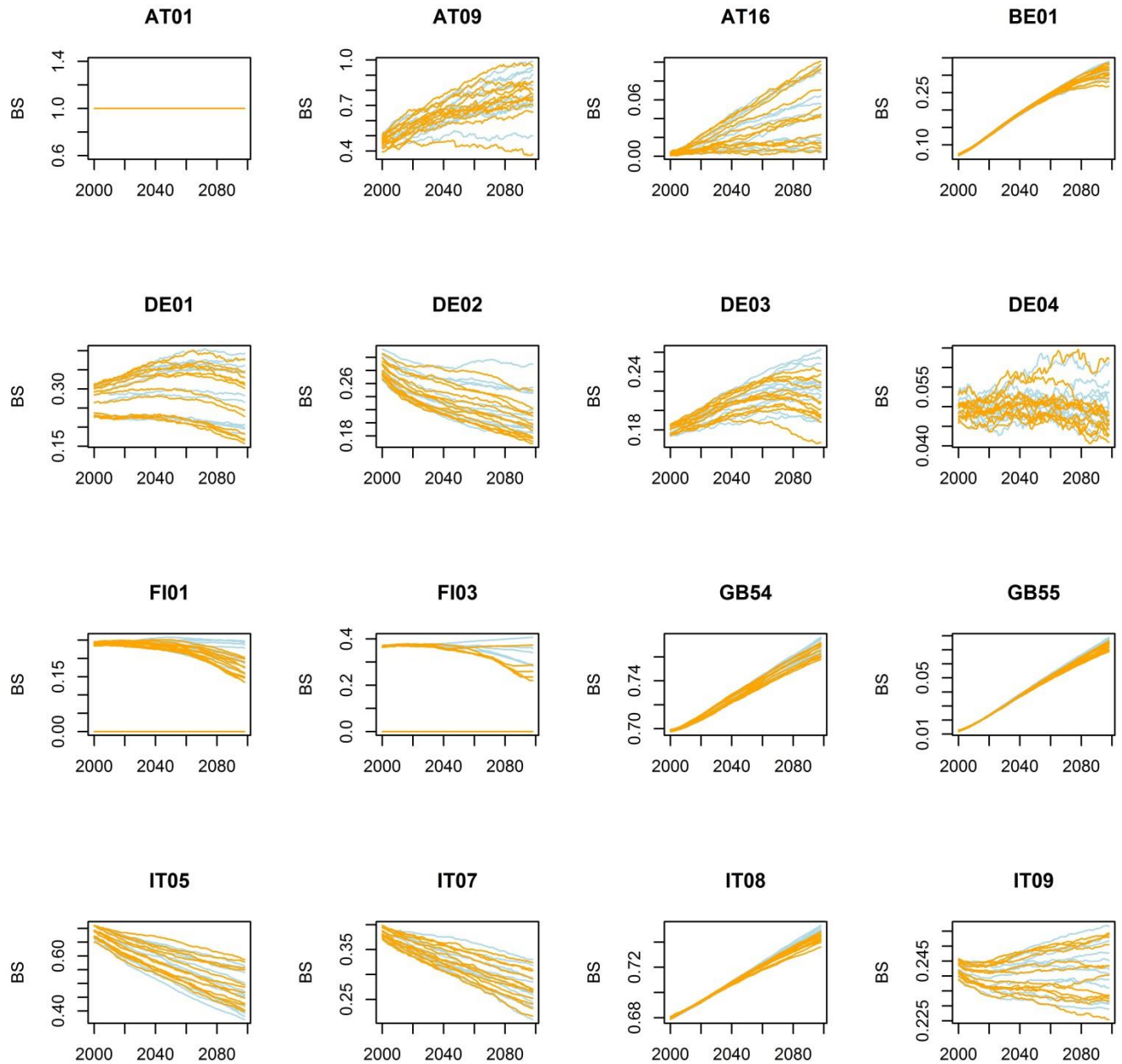
Supplementary Figure A7a. Time plots of simulated soil base saturation (BS, fraction $0 - 1$) with 24 climate change scenarios, twelve representing climate forcing level RCP4.5 (light blue) and twelve RCP8.5 (orange). BE01 is BE001, DE03 is DE301 and DE04 is DE507.
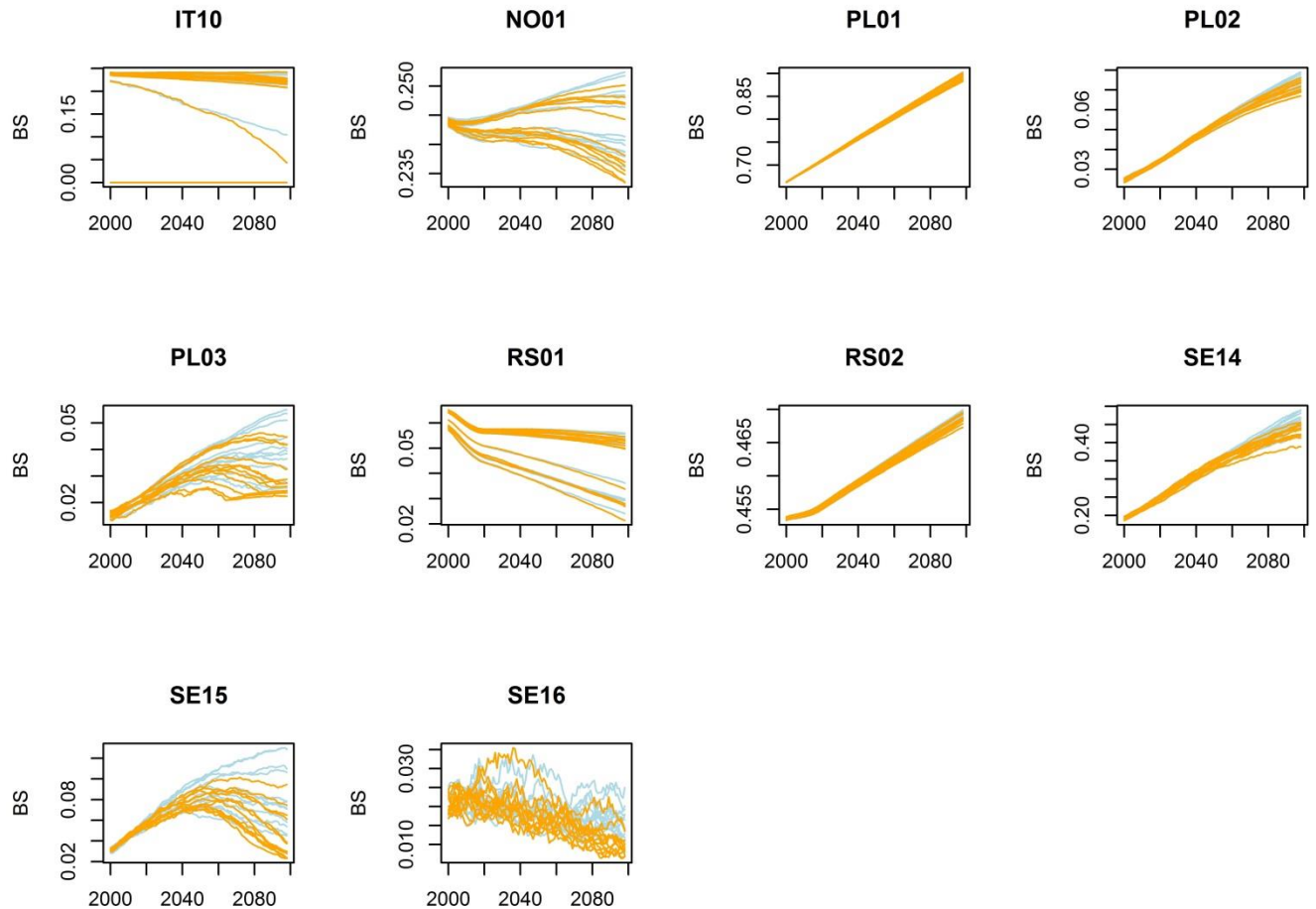
Supplementary Figure A7b. Time plots of simulated soil base saturation (BS, fraction $0-1$) with 24 climate change scenarios, twelve representing climate forcing level RCP4.5 (light blue) and twelve RCP8.5 (orange). PL02 is PLSNP and PL03 is PLTNP.
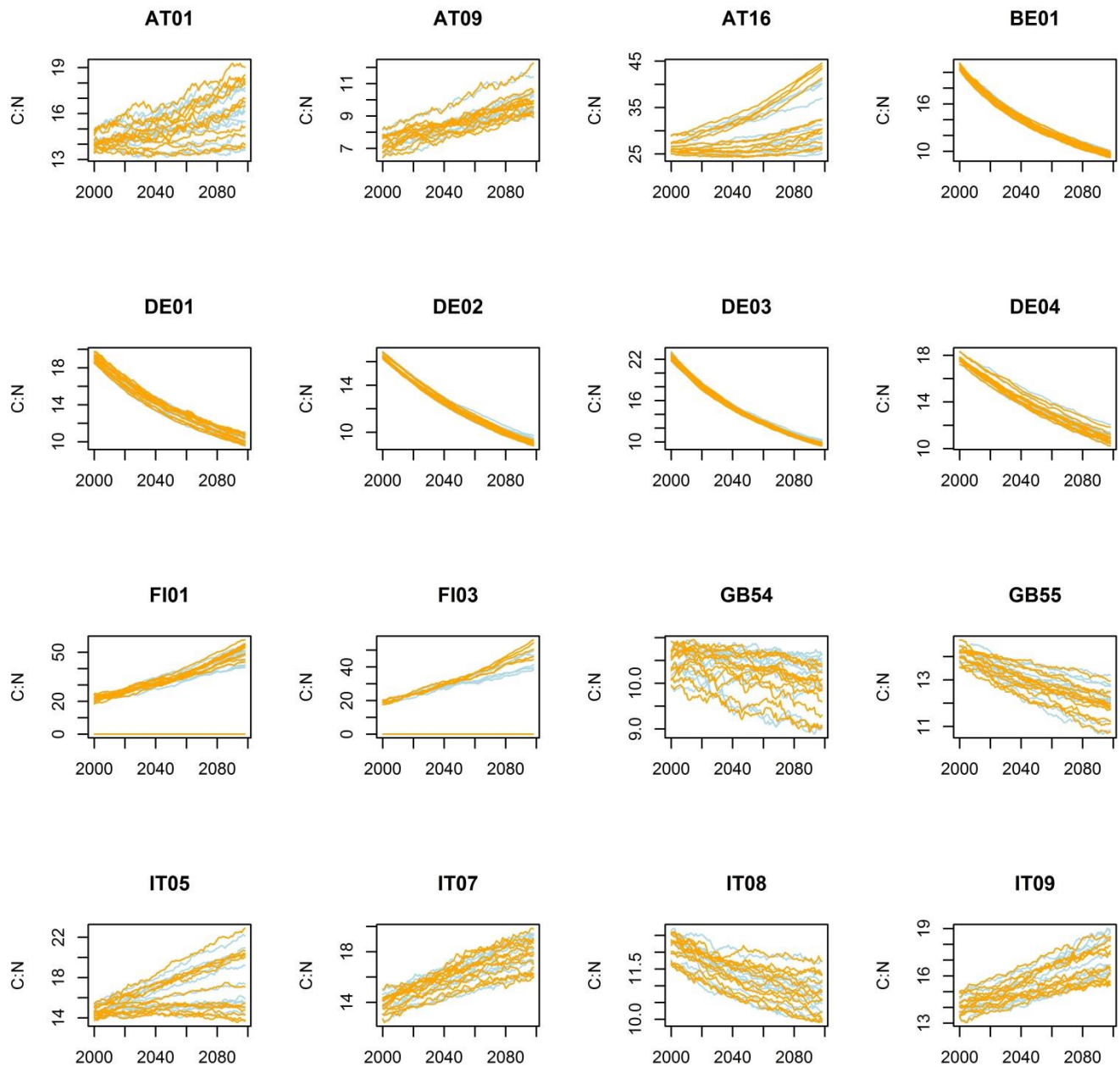
Supplementary Figure A8a. Time plots of simulated soil carbon to nitrogen ratio (C:N g g^{-1}) with

24 climate change scenarios, twelve representing climate forcing level RCP4.5 (light blue) and

twelve RCP8.5 (orange). BE01 is BE001, DE03 is DE301 and DE04 is DE507.
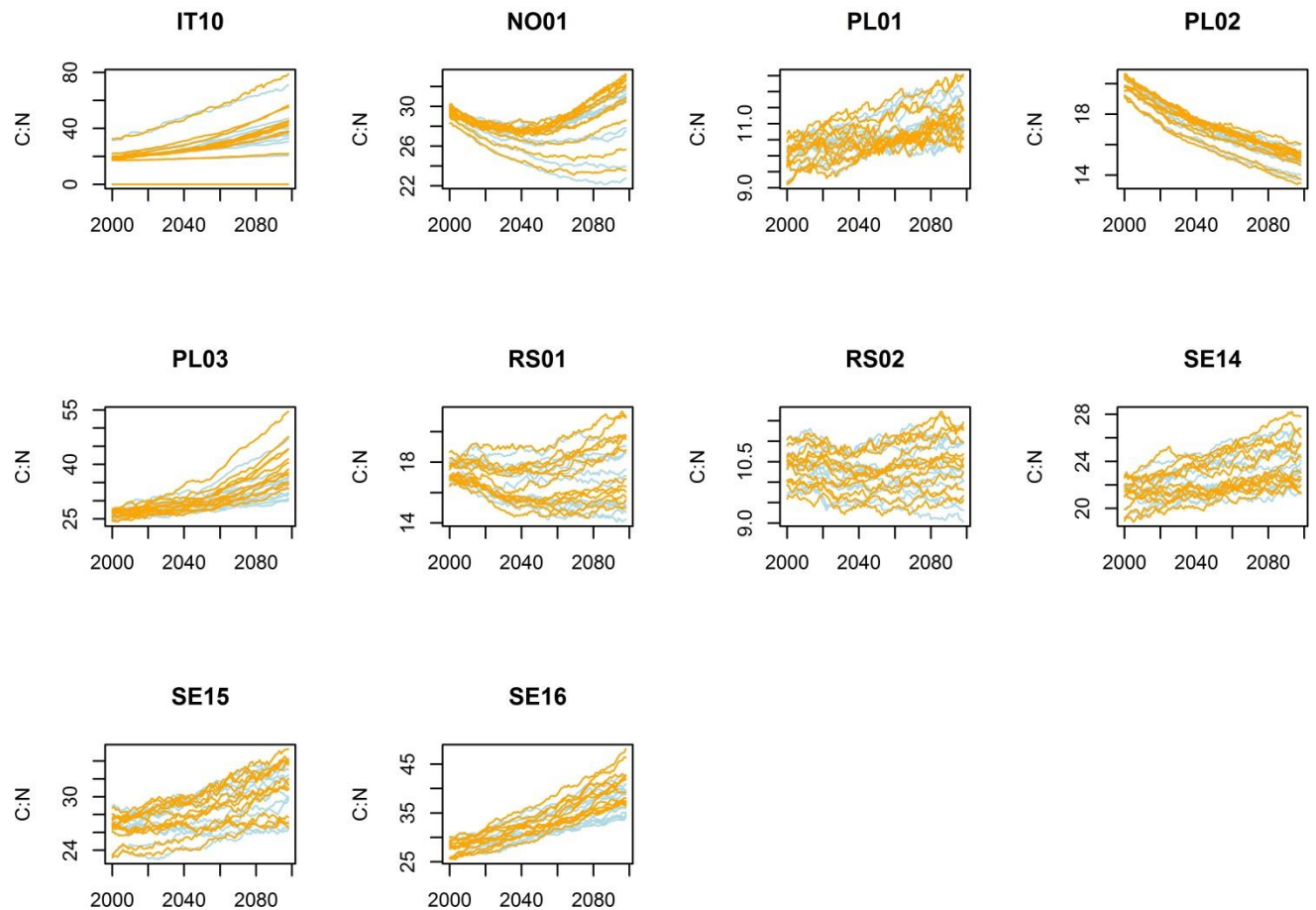
Supplementary Figure A8b. Time plots of simulated soil carbon to nitrogen ratio (C:N g g^{-1}) with 24 climate change scenarios, twelve representing climate forcing level RCP4.5 (light blue) and twelve RCP8.5 (orange). PL02 is PLSNP and PL03 is PLTNP.
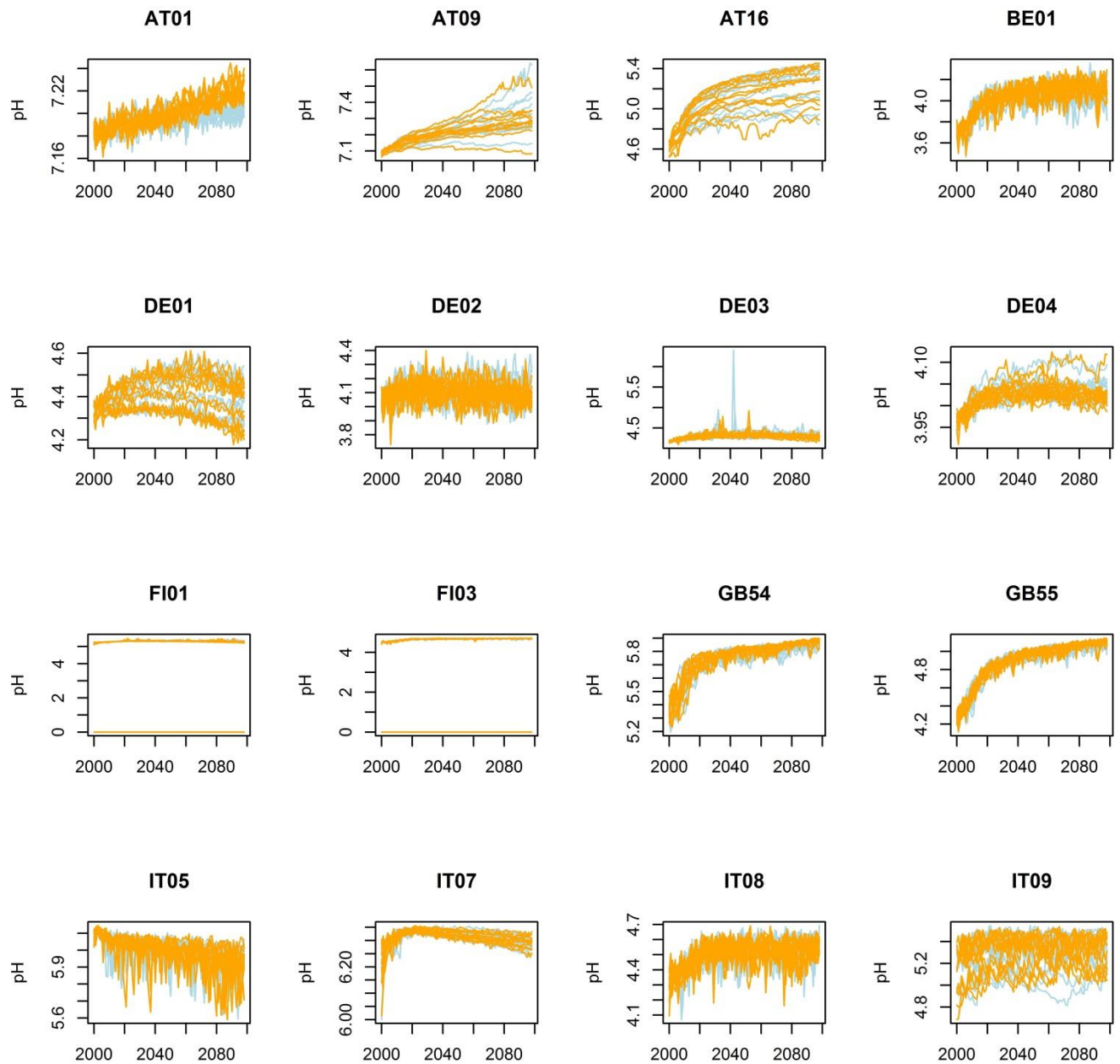
Supplementary Figure A9a. Time plots of simulated soil solution pH with 24 climate change scenarios, twelve representing climate forcing level RCP4.5 (light blue) and twelve RCP8.5 (orange). BE01 is BE001, DE03 is DE301 and DE04 is DE507.
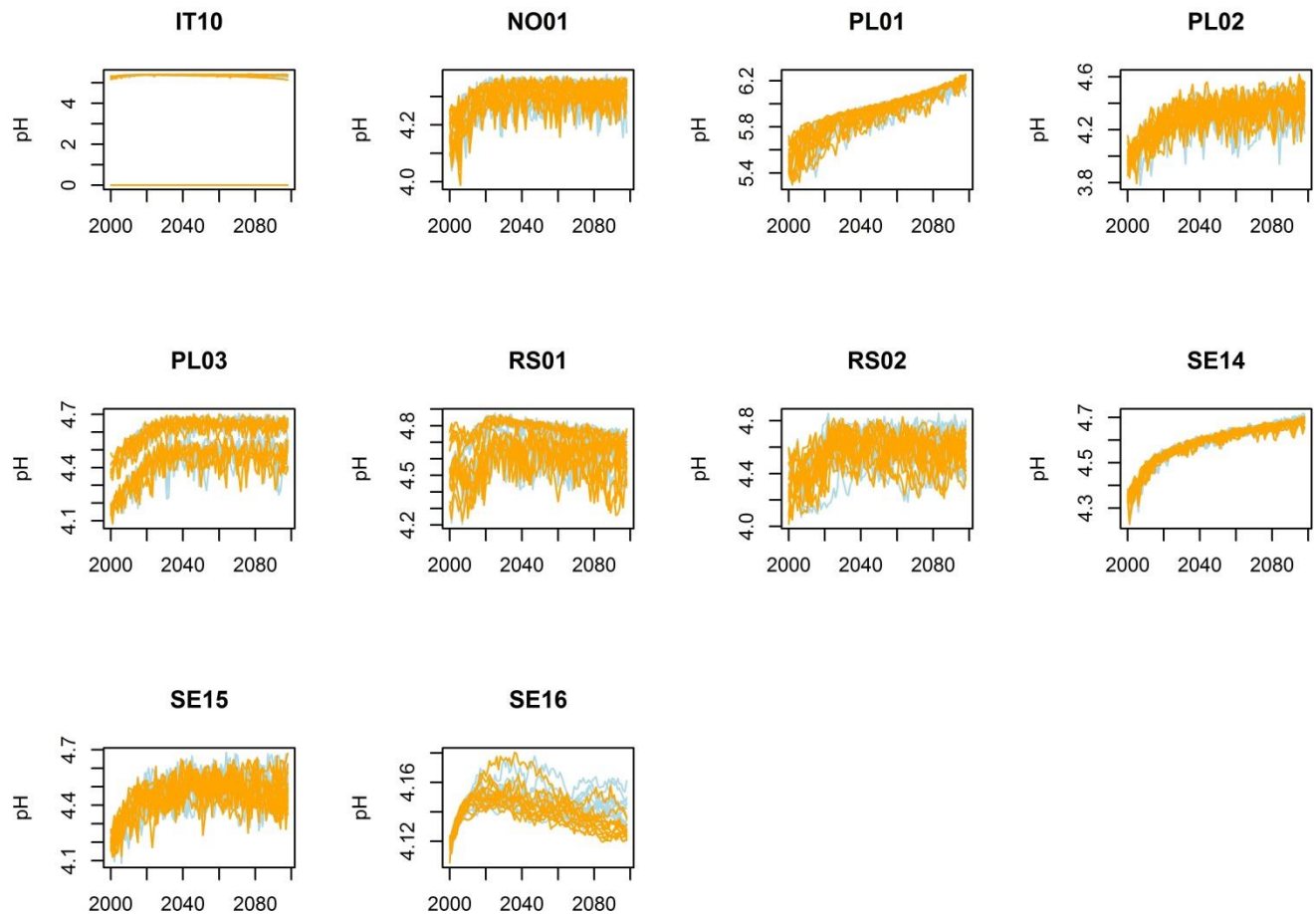
Supplementary Figure A9b. Time plots of simulated soil solution pH with 24 climate change scenarios, twelve representing climate forcing level RCP4.5 (light blue) and twelve RCP8.5 (orange). PL02 is PLSNP and PL03 is PLTNP.